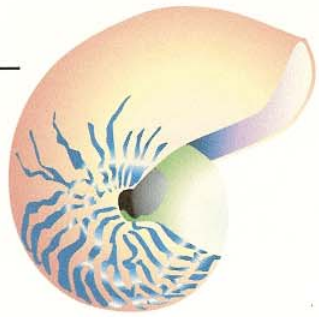

Coastal Marine Institute

University of Alaska

Seasonality of Boundary Conditions for Cook Inlet, Alaska

Steve Okkonen
Principal Investigator

Co-principal Investigators:
Scott Pegau
Susan Saupe

Final Report
OCS Study MMS 2009-041

August 2009

Minerals Management Service
Department of the Interior

and the

School of Fisheries & Ocean Sciences

University of Alaska Fairbanks

This study was funded in part by the U.S. Department of the Interior, Minerals Management Service (MMS) through Cooperative Agreement No. M08AR12674, originally numbered as Cooperative Agreement No. 0102CA85294, Task Order No. 37628, between MMS, Alaska Outer Continental Shelf Region, and the University of Alaska Fairbanks.

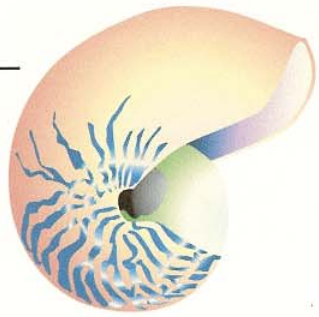

Coastal Marine Institute

University of Alaska

Seasonality of Boundary Conditions for Cook Inlet, Alaska

Steve Okkonen
Principal Investigator

Co-principal Investigators:
Scott Pegau
Susan Saupe

Final Report
OCS Study MMS 2009-041

August 2009

Minerals Management Service
Department of the Interior

and the

School of Fisheries & Ocean Sciences

University of Alaska Fairbanks

Contact information

Coastal Marine Institute
School of Fisheries and Ocean Sciences
University of Alaska Fairbanks
P. O. Box 757220
Fairbanks, AK 99775-7220

email: sharice@sfos.uaf.edu
phone: 907.474.7208
fax: 907.474.7204

TABLE OF CONTENTS

List of Figures.....**2**

List of Appendices.....**5**

Abstract.....**6**

Project Organization.....**7**

Introduction.....**7**

Methods.....**13**

Results.....**17**

Discussion.....**46**

Summary.....**54**

Acknowledgements.....**54**

Study Products.....**55**

References.....**56**

LIST OF FIGURES

Figure 1. Each yellow dot represents a sampling station along a transect line (circled numbers). Red dots are the locations of moorings added as part of this program.....**9**

Figure 2. Sampling stations are shown on the bathymetry.....**10**

Figure 3. Plots of monthly average wind speed (top) and vector-averaged direction (bottom) at the Augustine (solid line) and Drift River (dotted line) NDBC C-MAN stations are provided.....**11**

Figure 4. The first panel shows the circulation pattern in lower Cook Inlet presented by Burbank (1977) and the second panel is the pattern proposed by Muench et al. (1978).....**12**

Figure 5. Pictured is the CTD used on most cruises.....**14**

Figure 6. River discharge data for the Susitna River in upper Cook Inlet is shown.....**18**

Figure 7. Plotted are the temperature measurements since 1990 made at the Seldovia and Kodiak tide stations.....**19**

Figure 8. The plots are the fitted mean salinity (top left), the salinity amplitude (top right), the day of the minimum salinity (lower left), and the standard error of the fit (lower right) for line 5.....**21**

Figure 9. Fitted salinity data for line 4 is presented with the same order as figure 8.....**22**

Figure 10. Fitted salinity data for line 3 is presented with the same order as figure 8.....**23**

Figure 11. Fitted salinity data for line 2 is presented with the same order as figure 8.....**24**

Figure 12. Fitted salinity data for line 1 is presented with the same order as figure 8.....**25**

Figure 13. The plots are the fitted mean temperature (top left), the temperature amplitude (top right), the day of the maximum temperature (lower left), and the standard error of the fit (lower right) for line 5.....**27**

Figure 14. Fitted temperature data for line 4 is presented with the same order as figure 13.....**28**

Figure 15. Fitted temperature data for line 3 is presented with the same order as figure 13.....**29**

Figure 16. Fitted temperature data for line 2 is presented with the same order as figure 13.....**30**

Figure 17. Fitted temperature data for line 1 is presented with the same order as figure 13.....**31**

Figure 18. April salinity (left column) and temperature (right column) contour plots are shown.....**32**

Figure 19. September salinity (left column) and temperature (right column) contour plots are shown.....**33**

Figure 20. Minimum geostrophic currents are observed in May.....**34**

Figure 21. Maximum geostrophic currents are observed in September.....**35**

Figure 22. Freshwater transport by the geostrophic currents across lines 1 through 4 are provided.....**36**

Figure 23. Water levels at Seldovia during the 2006 spring-neap tide measurement sequence are provided with the sampling period outline in blue.....**36**

Figure 24. Salinity contours along line 1 are displayed in the left panel and temperature in the right.....**38**

Figure 25. Salinity contours along line 6 (Cape Adams to Cape Douglas) are displayed in the left panel and temperature in the right.....**39**

Figure 26. Salinity contours along line 7 (Magnet Rock to Mt. Augustine) are displayed in the left panel and temperature in the right.....**40**

Figure 27. Salinity contours along line 3 are displayed in the left panel and temperature in the right.....**41**

Figure 28. Salinity contours measured during 2005 by the Alaska Department of Fish and Game Offshore Test Fisheries program.....**42**

Figure 29. Salinity and depth data collected by a mooring on the eastern shelf of Kennedy Entrance is presented.....**44**

Figure 30. A short segment of the data presented in figure 29 is presented to show the fluctuations in salinity with tide stage.....**45**

Figure 31. Salinity contours along lines 1 and 2 are provided in the top panel and temperature is in the lower panel.....**48**

Figure 32. Temperature -salinity plots for April along line 1 (Kennedy), line 2 (Shelikof), line 3 (Anchor), line 4 (Barabara) showing that line 4 has a different characteristic than the other Cook Inlet waters.....**49**

Figure 33. Sea surface temperature image of Cook Inlet is shown.....**50**

Figure 34. A SeaWiFS chlorophyll image of lower Cook Inlet is shown.....**51**

Figure 35. The inferred surface circulation pattern is shown.....**53**

LIST OF APPENDICES

Appendix 1. Station locations.....**57**

Appendix 2. Cruise dates.....**59**

ABSTRACT

In order to continue improving our understanding of the physical environment of lower and central Cook Inlet, Alaska and to augment recent MMS-funded observational and modeling efforts we monitored oceanographic conditions that measured the seasonal changes in hydrographic properties at the inflow and outflow boundaries in lower Cook Inlet and the northern Gulf of Alaska and investigated the mechanism(s) influencing the distributions of these properties. During 2004 to 2006 we collected hydrographic measurements along transect lines crossing: 1) Kennedy Entrance and Stevenson Entrance from Port Chatham to Shuyak Island; 2) Shelikof Strait from Shuyak Island to Cape Douglas; 3) Cook Inlet from Red River to Anchor Point; 4) Kachemak Bay from Barbara Point to Bluff Point, and 5) the Forelands from East Foreland to West Foreland. During the third year we added two additional lines; 6) Cape Douglas to Cape Adams, and 7) Magnet Rock to Mount Augustine. The sampling in 2006 focused on the differences in properties during the spring and neap tide periods.

Strong seasonal variations in temperature and salinity were observed along all of the transect lines. Temperature reflected seasonal changes in solar insolation whereas freshwater content reflected seasonal changes in snowmelt, runoff, and precipitation patterns. Seasonal changes in freshwater input through the Alaska Coastal Current (ACC) and river discharge into Cook Inlet most likely control the non-tidal circulation in the lower portion of Cook Inlet. The freshwater-driven circulation was highly modified by the large tides of Cook Inlet. This modification could be seen at all time scales down to the individual tide. Tidal mixing near the mouth of Kachemak Bay during spring tides altered the flow of freshwater into lower Cook Inlet. The resultant path of the ACC appears to be controlled by the interaction of the tides with the bathymetry.

Previous studies examined seasonal changes at depth using moored instrumentation or looked at hydrographic properties over a very limited portion of the year. This study adds to the previous work by providing the seasonal changes in hydrographic properties at the surface as well as at depth along several transect lines in lower and central Cook Inlet. This work is the first to examine the variability of hydrographic properties over a range of temporal cycles (days - seasonal) and provides our first understanding of the role of the spring-neap cycle on controlling the distribution of those properties.

The temperature and salinity gradients between and across lower and central Cook Inlet suggest five principal factors necessary for accurate numerical simulations of Cook Inlet hydrography and circulation. These conditions include accurate spatial and/or temporal representations of (1) freshwater discharges into Cook Inlet (e.g. Susitna River, Matanuska River, Kenai River, and other CI river discharges), (2) heat and salt fluxes through Kennedy Entrance (including ACC transport), Stevenson Entrance, Shelikof Strait, (3) bathymetry, (4) tidal forcing and (5) solar insolation. Although wind forcing is also an important forcing mechanism, it was not directly investigated as part of this project, nor its role readily discernable from the hydrographic data.

PROJECT ORGANIZATION

This project was conducted by Steve Okkonen, W. Scott Pegau, and Susan Saupe. There were two main geographic portions of this study. The central Cook Inlet study was led by Dr. Okkonen and the lower Cook Inlet study was led by Dr. Pegau. Differences of equipment and techniques make separating the description of methods by these geographic regions. Within each study area there were Conductivity-Temperature-Depth (CTD) hydrographic surveys and moored deployments of a CTD.

INTRODUCTION

Cook Inlet is an important water body in Alaska, nearly two thirds of Alaska's population lives along its shores and watershed. Its geology changes dramatically from the upper to the lower portion of the Inlet creating a diverse array of habitats and species in its waters. It is home to productive commercial and sport fishing activities. It also is the main transportation route for cargo into Alaska. Oil and gas exploration and production has occurred in the northern portion of the Inlet since the early 1960's. The management of resources within Cook Inlet requires an understanding of how it functions as a system.

Cook Inlet is a broad, long, and shallow embayment extending northward from the Gulf of Alaska into south-central Alaska (Figures 1 and 2). Several large rivers flow into the northern (upper) section of Cook Inlet. Discharges from these rivers have large seasonal variability with high flows associated with snowmelt in the spring and storm events in the fall. The bathymetry shoals to less than 100 m near the mouth of Cook Inlet. A deeper channel extends along the axis of the Inlet, and has branches into Kachemak Bay and around Kalgin Island. The shape and depth of Cook Inlet is such that the M2 tide resonates leading to a very large tidal amplitude. The Inlet is narrower towards the north causing the tidal amplitude and resulting currents to increase towards the constriction formed by the Forelands. Changes in tidal flow associated with the changes in bathymetry forms strong shear and convergence zones locally known as rips. These rips accumulate debris, ice, and oil, as was demonstrated in the 1987 T/V Glacier Bay oil spill.

Winds in Cook Inlet are largely driven by the strength and position of the Aleutian Low and the mountainous terrain surrounding the Inlet. In the winter the Inlet winds are driven by the cyclonic flow around the Aleutian Low (MMS EIS 2003) and generally are from the north and northeast (Figure 3). During the summer the Inlet winds are more often from the south and southwest, driven in part by the temperature gradient from land to the ocean. Stronger winds form in areas with gaps in the mountains, such as in Kamishak Bay where mountains funnel air in a southeast direction through Kamishak Bay and across the Barren Islands. Winds weaken in central Cook Inlet.

Much of our understanding of the circulation of the lower portion of Cook Inlet comes from studies conducted in the 1970's (Burbank 1977, Barrick 1978, Muench et al. 1978, Muench et al. 1981). These investigators used hydrographic surveys, current meter moorings, drifters, satellite images, and high-frequency radar to infer the circulation. Most of these studies focused on the spring and summer, with the exception of Muench et al. 1981, which looked at summer and winter circulation using moored sensors. Although the studies were conducted during a similar time frame, there are significant differences in the inferred circulation proposed by Burbank (1977) and Muench et al. (1978). The primary differences in the two studies are the path of the ACC and the path of freshwater flowing out of Cook Inlet along the western side (Figure. 4).

Recently a number of studies have been conducted in Cook Inlet. Two workshops have been held that produced proceedings that describe the modern research (Johnson and Okkonen 2000, Schumacher 2005) which includes a pair of temperature and salinity studies that are precursors to this work (Okkonen and

Howell 2003, Okkonen 2004). Other recent work has focused on the interactions between the physical and biological properties (Speckman et al. 2005) and modeling of upper Cook Inlet (Oey et al. 2007). During the period of this work there were several other activities to improve our understanding of circulation in Cook Inlet. A group led by Mark Johnson from the University of Alaska Fairbanks (UAF) released drifters at the northern portion of our study area and worked on improving the 3-dimensional models. The National Oceanic and Atmospheric Administration (NOAA) placed several acoustic doppler current profiler (ADCP) moorings in the Inlet to improve the tidal current predictions. Alaska Department of Fish and Game (ADF&G) began profiling measurements of oceanographic properties in association with the offshore test fishery program conducted through July. Both NOAA and UAF investigators installed high-frequency radar units to map surface currents. A more complete description of recent efforts can be found on the internet (http://doc.aoos.org/other_meetings/2005/cook_inlet_physical_oceanography_workshop_proceedings-combined%20sections-final-2006.pdf) which includes the proceedings of a Physical Oceanography of Cook Inlet workshop held as part of this project.

In this work we examine the variability in hydrographic properties at time scales of seasons to days, how that variability is forced, and the implications for circulation in the area. The descriptions of oceanic properties provided here also provide boundary conditions necessary for numerical circulation models currently existing (*e.g*. CIRCAC and NOAA HAZMAT) and under development (*e.g.* CMI-funded model by Mark Johnson, or the Regional Ocean Model by Alaska Ocean Observing System).

Figure 1. Each yellow dot represents a sampling station along a transect line (circled numbers). Red dots are the locations of moorings added as part of this program. The Offshore test fishery data comes from the center of line 3. Lines 1, 2, and 5 demark the boundaries of lower and central Cook Inlet, with line 3 separating lower and central Cook Inlet.

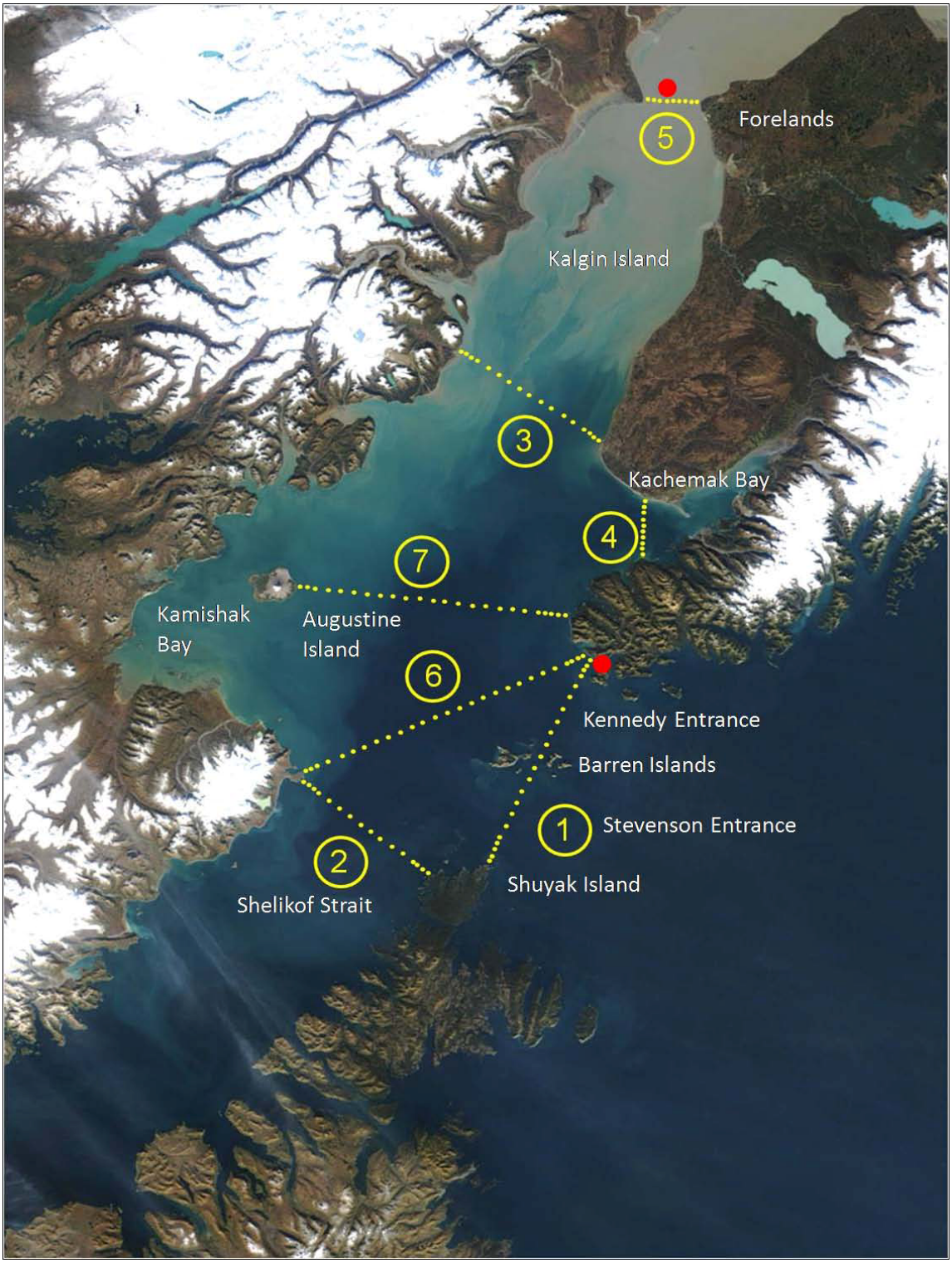

Figure 2. Sampling stations are shown on the bathymetry. Red bathymetry is shallow and dark blue is approximately 200 meters depth. The 100m isobath occurs at the transition from yellow to blue.

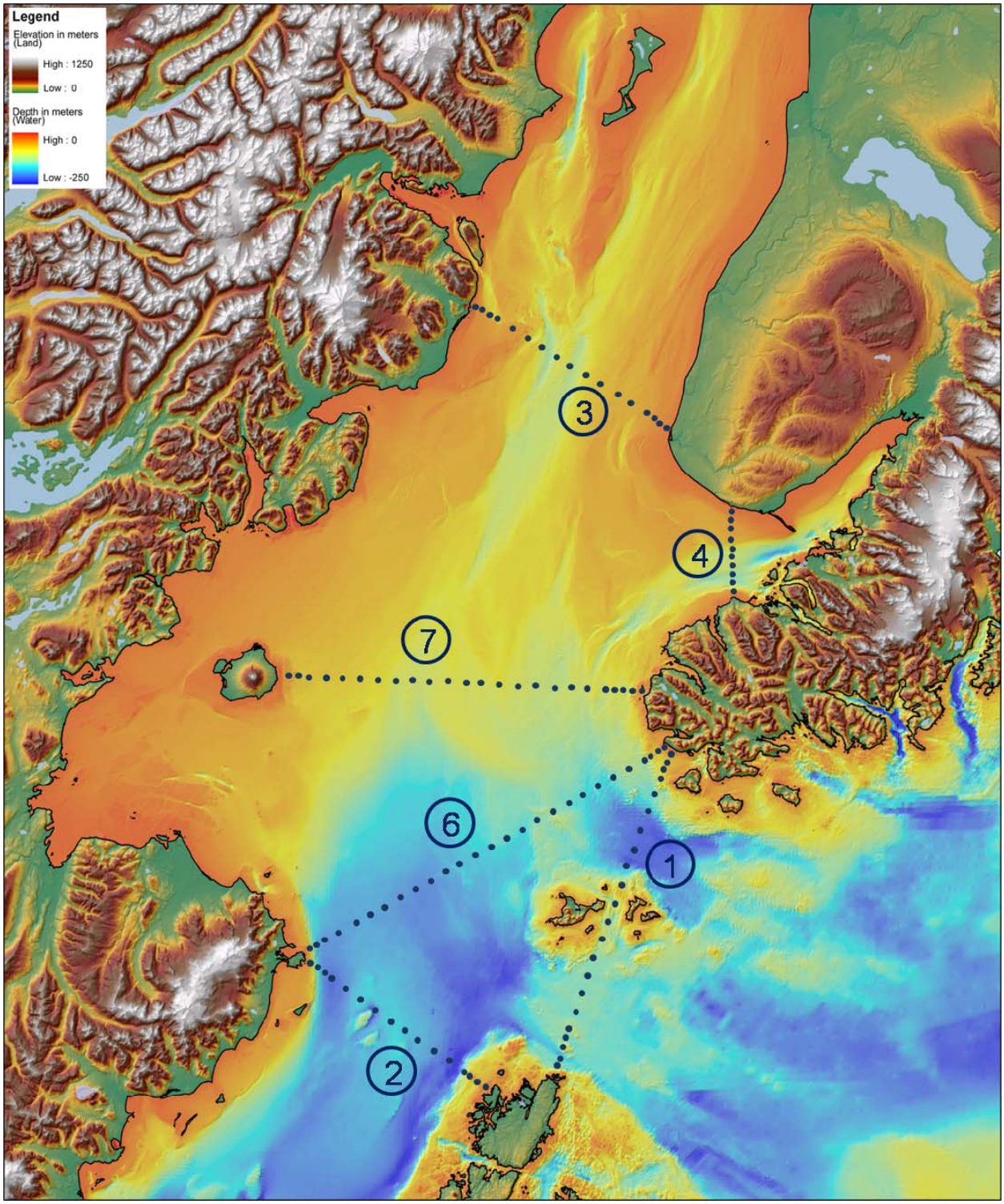

Figure 3. Plots of monthly average wind speed (top) and vector-averaged direction (bottom) at the Augustine (solid line) and Drift River (dotted line) NDBC C-MAN stations are provided. Augustine is within Kamishak Bay in lower Cook Inlet and Drift River is in central Cook Inlet.

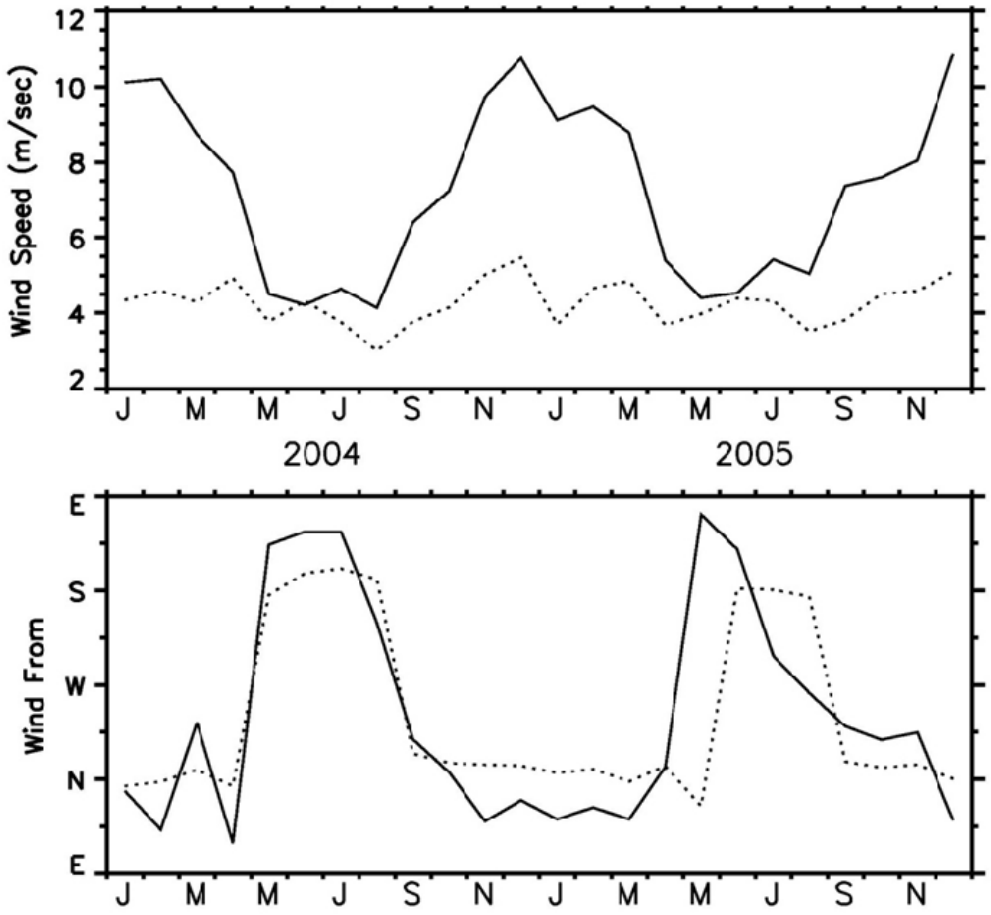

Figure 4. The first panel shows the circulation pattern in lower Cook Inlet presented by Burbank (1977) and the second panel is the pattern proposed by Muench et al. (1978).

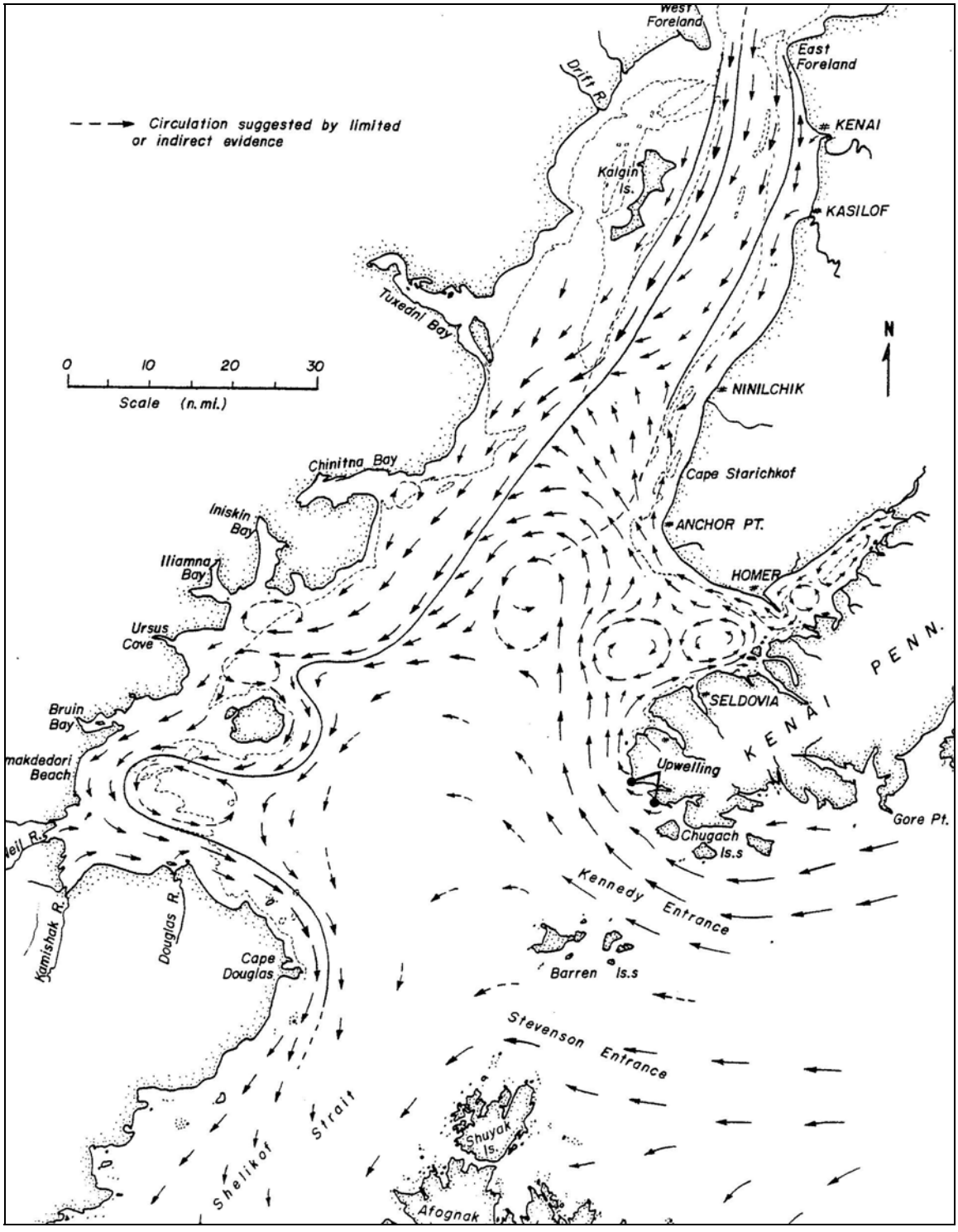

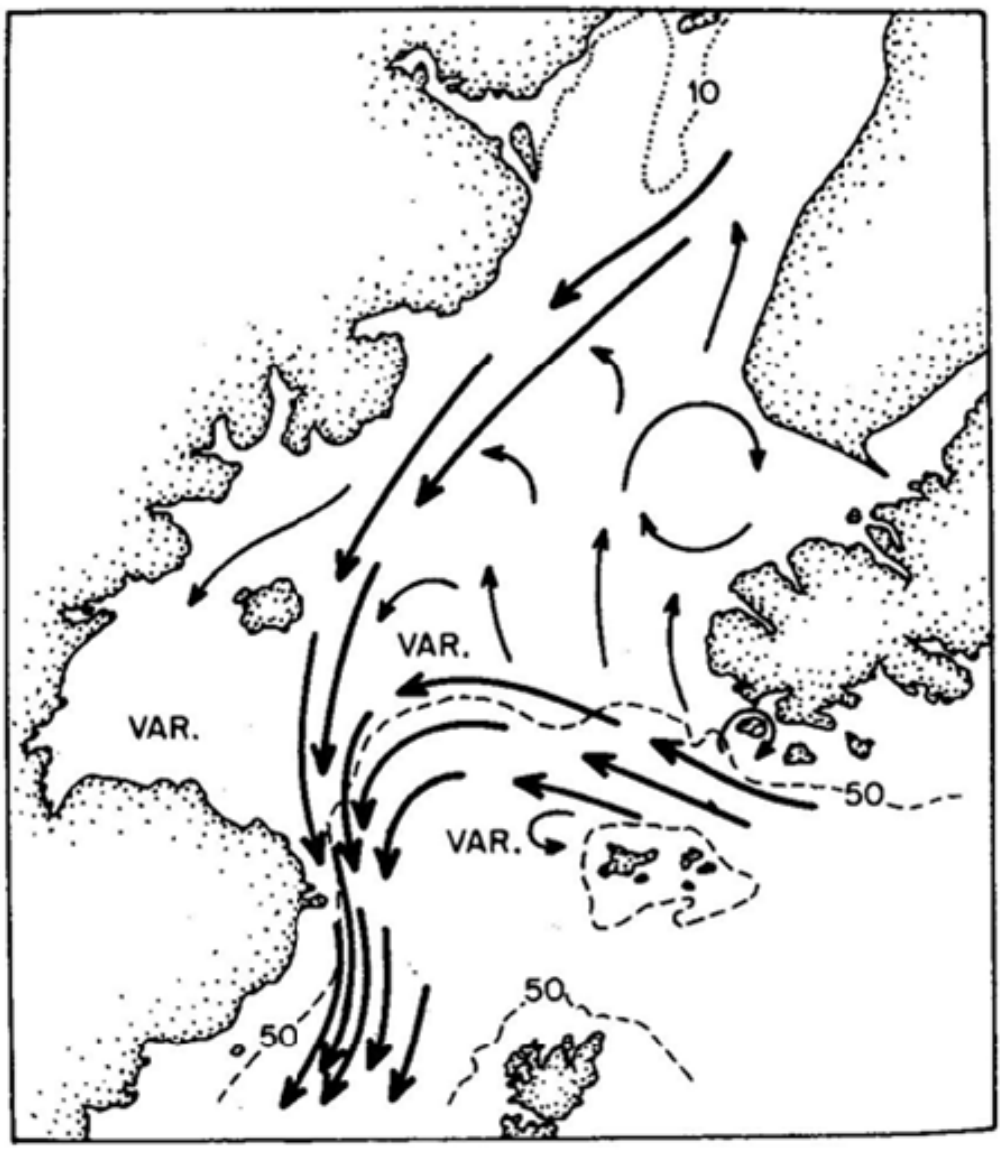

METHODS

Conductivity-temperature-depth (CTD) hydrographic surveys were conducted along seven transect lines (Figure 1 and Appendix 1) in Cook Inlet. Each survey was conducted using a SeaBird Electronics SBE-19+ CTD with ancillary sensors (Figure 5). Survey dates and frequency of sampling were different between the two regions because of weather and scheduling constraints. The survey dates are provided in Appendix 2.

Figure 5. Pictured is the CTD used on most cruises. The rope below goes to a weight that was used to reduce flagging in fast current regimes.

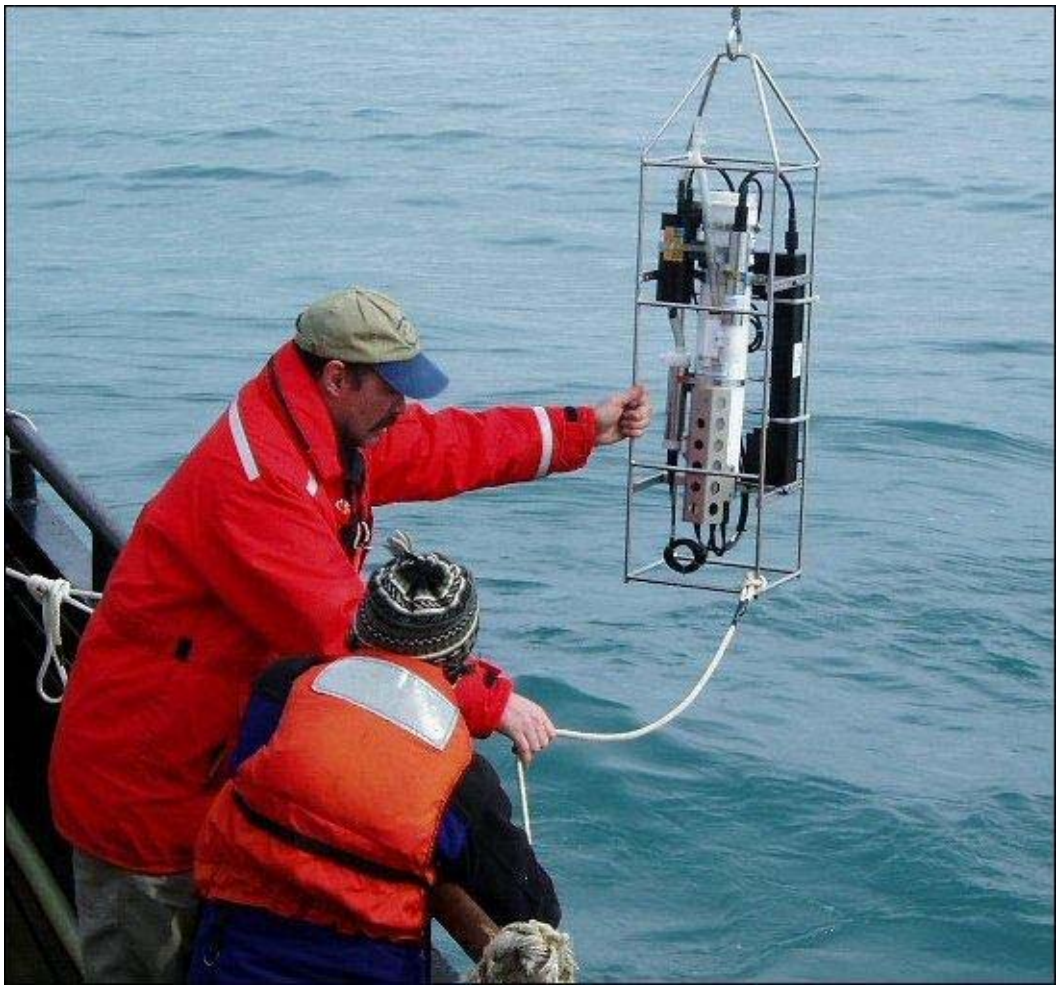

Lower Cook Inlet Hydrographic Surveys

The CTD surveys were conducted six times in 2004 and 2005, and four times in 2006. In 2004 and 2005 only lines 1 through 4 were occupied. In 2006 lines 6 and 7 were added in lower Cook Inlet to determine the location where the ACC crosses Cook Inlet. Line 5 survey characteristics are described below in the Central Cook Inlet Hydrographic Surveys section. In 2003 we focused on the spring and summer season with cruises in April, May, June, July, August, and September. In 2004 we included fall and winter with surveys in January, April, June, July, September, and October. We tried to conduct surveys during neap tides when possible to allow the CTD to reach greater depths. The exact date of each cruise was primarily dictated by having a period of two days where the expected wind speed was 15 knots or less and seas less than seven feet. These conditions were desired for safety in deploying the equipment from the smaller (~50 foot) vessels that were used. In 2006 we scheduled surveys to occur in the fall to coincide with high freshwater discharge. The cruises were scheduled during spring and neap tides to examine the role of the fortnightly tides on the distribution of hydrographic properties. It took just under two days to complete

lines 1 through 4, and an additional day to add lines 6 and 7. Depending on the weather, surveys were initiated on either line 1 or 3 and ended on line 4.

The survey lines were designed with stations spaced one nautical mile (nm) apart close to each shore and two nm apart farther offshore (Figure 2, Appendix 1). Line 1 crossed Kennedy and Stevenson Entrances, passing between the Barren Islands midway along the line. Line 1 consisted of 22 stations. Line 2 consisted of 16 stations across Shelikof Strait. Line 3 ran just north of the confluence of Cook Inlet and Kachemak Bay between the Anchor and Johnson Rivers. Line 4 had 10 stations spaced one nm apart between Barabara and Bluff Points in Kachemak Bay. Line 6 included 27 stations extending across the mouth of Cook Inlet between Cape Adams and Cape Douglas. Lastly, line 7 had 24 stations extending between Magnet Rock and Augustine Island. The water depth along this line averages approximately 75 meters, considerably less than the depth along line 6.

The SBE-19+ CTD and ancillary sensors were placed in a cage and a 5 -10 Kg weight on a 1-m long line was hung beneath the cage (Figure 5). The purpose of the weight was to help reduce the flagging of the cage in the strong currents and to provide an indication when the cage neared the bottom. At each station the CTD was started and allowed to soak a couple meters below the surface for one minute before starting a profile. The CTD was lowered at approximately 0.5 m s^{-1} until it hit the bottom or the line was completely let out (200 m). The CTD was retrieved at one m s^{-1} or faster.

The data were downloaded at the end of each sampling trip and processed using standard SeaBird processing algorithms. The data were first run through Datcnv to apply the calibration coefficients. The Filter algorithm was applied using manufacturer recommended filter constants. Plumbing lags were applied using Alignctd. The lags were determined each year by examining up and downcasts and getting them to align. Alignment was also constrained by preventing salinity and density spikes in the final data set. The Loopedit algorithm was applied to only keep data when the sensor was descending. The salinity, density, and depth were then calculated using the Derive algorithm. The data were then binned into 1-m depth bins using only the downcast data and the Binavg algorithm and then output in an ASCII tabular format.

All of the ASCII data from a given cruise were combined into a single spreadsheet and the cruise number, station number, date, time, latitude, longitude, and station depth were added to the data from each station. These cruise data sheets were then used in the plotting and analysis of the data, and were submitted the National Ocean Data Center and to the Alaska Ocean Observing System for inclusion in their databases.

Lower Cook Inlet Mooring

The southern mooring consisted of a SeaBird Microcat CTD recorder mounted on the top of a 2X2 m crab pot that had the webbing stripped off. The mooring was placed on the shelf just west of Kennedy Entrance (59° 12.161N 151° 50.860W). The mooring location was chosen to avoid the strong currents in Kennedy Entrance and the need to protect the mooring from storms. The mooring was deployed on August 12, 2006 and retrieved on October 28, 2006. The instrument was retrieved to prevent damage by the strong winter storms that occur in the area. The Microcat was programmed to collect an average five samples every 15 minutes. The raw data were collected in Alaska Standard Time and then converted to UTC.

While this program did not have a mooring component that covers the entire sampling period, it is important to have some measure of the interannual variability. One source of oceanographic data is from the NOAA tide stations in Kodiak and Seldovia, which are just outside of the study region. The data can be found on the NOAA website.

(http://tidesandcurrents.noaa.gov/station_retrieve.shtml?type=Meteorological%20Observations) The six-minute water temperature data were averaged to provide a monthly water temperature record.

Central Cook Inlet Hydrographic Surveys

A Sea-Bird Electronics, Inc. SBE 19+ Profiler CTD was used to acquire surface-to-bottom measurements of temperature and salinity during surveys along an east-west transect (latitude 60° 43'N) between the East Foreland and West Foreland (line 5) in central Cook Inlet, Alaska (Figure 1). Five surveys were conducted along this transect between May and October in 2004 and four surveys were conducted from May to October in 2005. These surveys generally occurred during mid-to-late stages of the flood tide (predominantly northward-flowing surface currents). Two additional surveys were conducted on 9 August 2006 to compare hydrography across the Forelands transect during flood and ebb. The survey dates are listed in Appendix 2.

Sampling along each crossing of the 14.5-km (~8 nm) Forelands transect generally took a little less than 1.5 hours. Successive CTD casts were separated by 2 minutes of longitude (~1.81 km; ~1 nm). Cast locations were acquired from a vessel-mounted GPS unit. The CTD was lowered at approximately 0.5 m s^{-1} and individual measurements of temperature, salinity, and pressure were acquired at a rate of four per second. Temperature, salinity, and density (sigma-t) data from each downcast were averaged in 1-m bins centered on integer depths.

Central Cook Inlet Mooring

A Sea-Bird Electronics, Inc. SBE 37-SM microcat CTD was deployed on a bracket attached to the leg of the XTO 'C' platform in central Cook Inlet (60° 45.7'N, 151° 30.3'W) on 11 August 2006 to acquire time series measurements of near-surface temperature and salinity. The XTO platform lies 5 km north of the Forelands transect. Subsequent inspection of the bracket on 28 August 2006 showed that the bracket had become loose and the microcat was removed. Data were collected every 15 minutes during the deployment.

Further processing

To determine the seasonal changes each depth bin (z) of the CTD data from each station (x) of the 16-cruise time series were fit using least squares to the sinusoidal function

$$F(x,z,t) = A\cdot\cos(2\pi\cdot t/365) + B\cdot\sin(2\pi\cdot t/365) + C\cdot t + D$$

from which two-year mean temperatures, salinities, and densities at each CTD station and integer depth were calculated according to

$$\bar{F}(x,z) = \frac{\int_{t=0}^{t=730} F(x,z,t)dt}{\Delta T}.$$

In this formulation, t = 0 corresponds to 1 January 2004. The amplitudes and phases of the annual period temperature, salinity, and density signals at each CTD station and integer depth were determined from the corresponding least squares coefficients, where amplitude = $(A^2 + B^2)^{1/2}$, and phase = $\tan^{-1}(B/A)$.

Surface geostrophic currents were estimated from the hydrographic transects. This was accomplished by calculating geopotential anomalies (or dynamic heights, ($\Delta\Phi_A$)) at location (A) using:

$$\Delta\Phi_A = \int_{P_{1A}}^{P_{2A}} \delta dp$$

where δ is the specific volume anomaly, which is integrated between pressure surfaces. The surface velocity is estimated from the slope of the ocean surface calculated using:

$$v = \frac{1}{f}\frac{\Delta\Phi_B - \Delta\Phi_A}{L}$$

where v is the velocity perpendicular to the transect line, f is the coriolis parameter, and L is the distance between points A and B. We assumed a level of no motion at 100 m for our calculations.

Freshwater content was determined using a mixing model, $F_{fw} = 1 - \frac{S_{meas}}{S_{ref}}$, where F_{fw} is the fraction of freshwater, S_{meas} is the measured salinity, S_{ref} is the reference salinity, and the salinity of freshwater is assumed to be zero. We used 33.8 PSU as the reference salinity to be consistent with Weingartner et al. 2005. Combining the fraction of freshwater with the volume of water in a 1 meter wide section along the area of the transect we estimated the total freshwater in that volume.

Freshwater flux was estimated using the calculated geostrophic currents combined with the freshwater content estimates.

RESULTS

To provide a measure of inter-annual variability we examined the river discharge into upper Cook Inlet and water temperature data from the NOAA tide stations in Kodiak and Seldovia, which are just outside of the study region.

Freshwater input is important in determining the circulation within Cook Inlet. Unfortunately, only a few of the rivers are gauged for measuring discharge, and those measurements are not possible when the river is covered with ice. Discharge measurements on the Susitna River, the largest draining into upper Cook Inlet, shows a maximum discharge in May as the river first opens up (Figure 6, data from http://waterdata.usgs.gov/ak/nwis/rt). Through the summer there is considerable variability in the discharge associated with rainfall within the drainage basin, but in general the flow decreases from June through August and sometime in September it is dramatically reduced as snowmelt ceases and precipitation starts to be snow once again. This is in stark contrast to the more coastal areas where freshwater input is at its maximum in September and October due to the fall storms (Royer, 1982).

The water temperature records show large seasonal and interannual variability (Figure 7). During the three years of sampling, similar temperatures were observed in 2004 and 2006. The summer of 2005, however; was the warmest on record at the Seldovia tide station and the third warmest in Kodiak. The seasonal temperature pattern is that the winter cold period lasts from December until March. Beginning at the end of March the temperature increases steadily through June. July through September is the warmest season and fall storms begin to bring down the temperature in October. The temperature drop in

the fall is dependent on storm activity so it tends to drop rapidly during these events, unlike the steady increase in temperature through the spring.

Figure 6. River discharge data for the Susitna River in upper Cook Inlet is shown. The red line is the measured discharge, and the blue line is the estimated discharge. Note that measured values are typically from the beginning of May to the end of September.

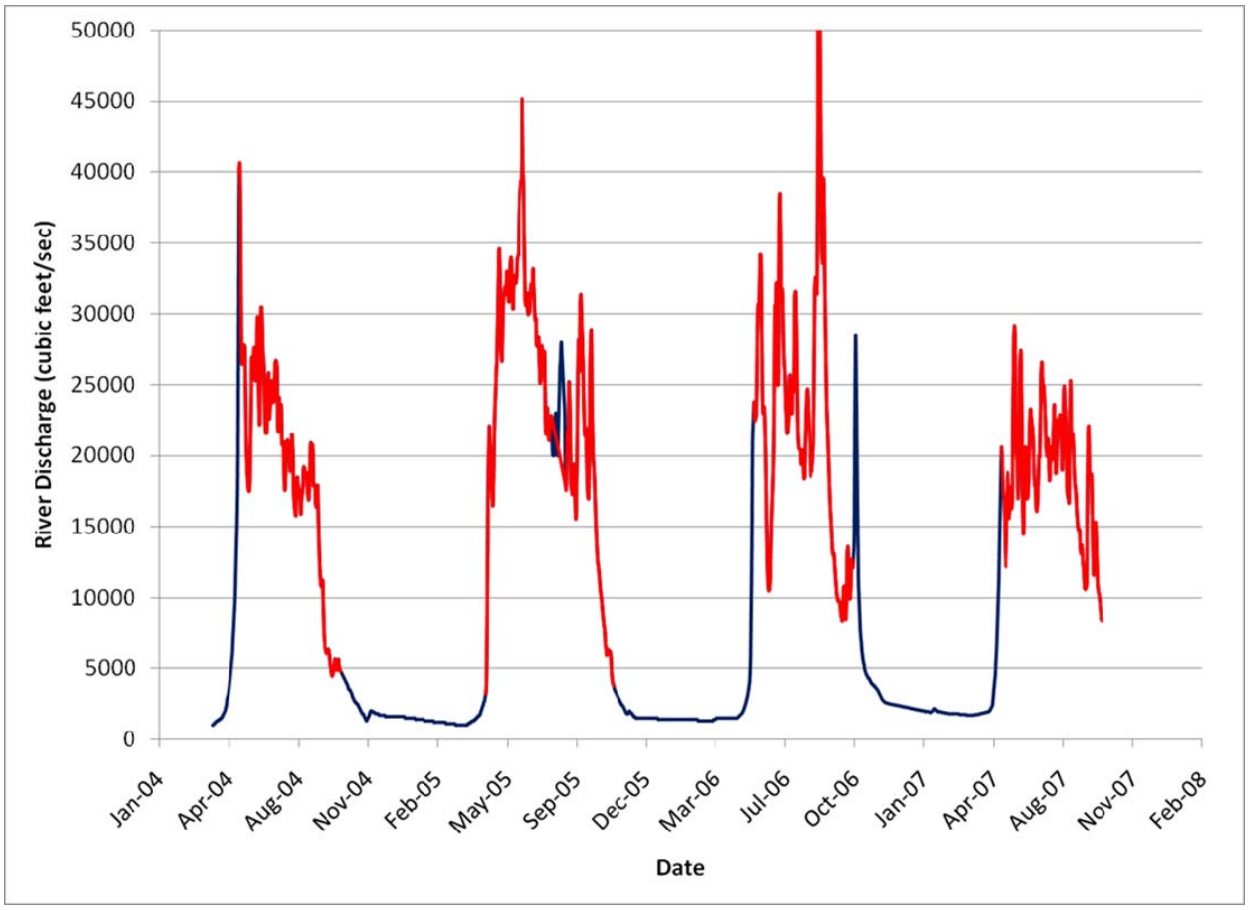

Figure 7. Plotted are the temperature measurements since 1990 made at the Seldovia and Kodiak tide stations.

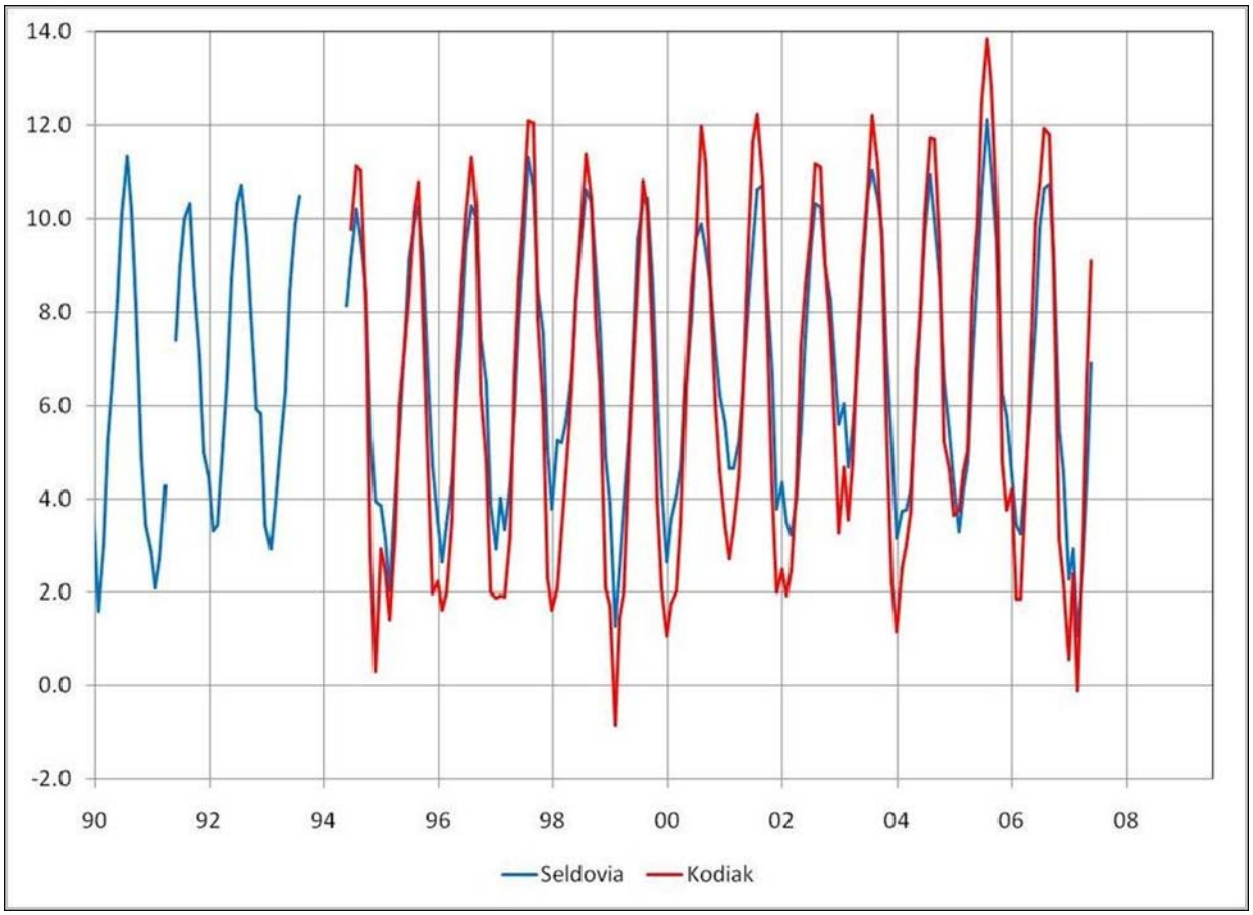

Mean conditions and seasonal variability of salinity

The seasonal cycles (mean, amplitude, phase, and standard error) of salinity along transect lines 1-5, as estimated using the least squares procedure described above, are summarized in Figures 8-12. Comparison of mean salinities from lines 1-5 broadly affirms the known north-south salinity gradient. Most of the largest rivers of the Cook Inlet watershed discharge to the Inlet north of the Forelands. Consequently, the lowest mean salinities (~26-28) and the largest amplitude seasonal salinity signal (~3) within the study occur between the Forelands (line 5; because CTD casts conducted during the March 2005 Forelands survey only went to ~30 m, least squares estimates were not computed for depths deeper than ~30 m). Mean salinities increase from west to east indicating a mean southward baroclinic flow in the upper part of the water column. The phase plot indicates that the highest salinities at the Forelands occur in mid-February when river discharge is low, while the lowest salinities occur six months later in mid-August, roughly coinciding with the middle of the summer discharge pulse (Figure 6).

About 100 km south of the Forelands, line 3 mean salinities range between ~29 and <31.5. The west-to-east inclination of isohalines on the western side of line 3 indicates mean southward baroclinic flow. The single isohaline contour on the eastern side of line 3 and its east-to-west inclination indicate a comparatively weaker northward (up inlet) mean flow on the eastern side of Cook Inlet. The salinity amplitude is >1 in the upper ~20 m on the west side of the Inlet and ~0.5 on the eastern side of the Inlet. The lowest salinities occur in September.

At line 2, roughly 120 km south of line 3, mean near-surface salinities are < 30.5 along the western side of the line and >31 along the eastern side of the line. The broad west-to-east inclination of the mean isohalines indicates that the mean baroclinic flow is directed southward, out of the Inlet into Shelikof Strait. The seasonal salinity amplitudes in the upper 20 m are ~0.7-1.2 on the west side of Shelikof Strait and ~0.5-1.1 on the eastern side of the strait. The lowest salinities occur in late September. The reader should note that, at depths greater than about 30 m, the standard errors of the least squares salinity estimates are comparable to the corresponding estimated amplitudes of the seasonal signal. This suggests that, given the relatively few surveys conducted, the phase estimates for the seasonal salinity signal at depths below 30 m are not reliable.

Mean salinities along line 1 are generally < 31.5 in the upper 20-m of the water column. The ventilation of the 31.5 isohaline near the midpoint and near the southern end of line 1 reflects enhanced (likely tidal-related) mixing in the vicinity of the Barren Islands and Shuyak Island, respectively. Salinities less than 31 at the northern end of line 1 reveal the presence of the ACC. Broadly speaking, the north-to-south inclination of the line 1 mean isohalines indicates westward baroclinic geostrophic flow (into lower Cook Inlet). The maximum salinity amplitude along line 1 (~0.8-1.2) occurs in the upper 20 m at the northern end of the line, coincident with the mean location of the ACC. Consistent with mooring-based measurements acquired near Seward (Weingartner et al., 2005), the phase plot indicates the lowest salinities occur late September-early October when ACC surface salinities are lowest. As was the case for line 2, phase estimates are not reliable at depths greater than ~30 m because standard errors are comparable to the corresponding estimated amplitudes of the seasonal signal.

Mean salinities along line 4 vary little (31.5-31.0) over most of the water column. The slope of the isohalines along line 4 indicate mean eastward baroclinic flow into Kachemak Bay near the southern end of the line and mean westward flow out of Kachemak Bay near the northern end of the line. The amplitude plot indicates that seasonal amplitudes are ~0.4-0.6 at depths >10 m for most locations. However, amplitudes markedly increase to > 1 in the upper 10 m along the northern half of the line. The phase plot indicates that this relatively fresh lens is most pronounced in September.

Figure 8. The plots are the fitted mean salinity (top left), the salinity amplitude (top right), the day of the minimum salinity (lower left), and the standard error of the fit (lower right) for line 5.

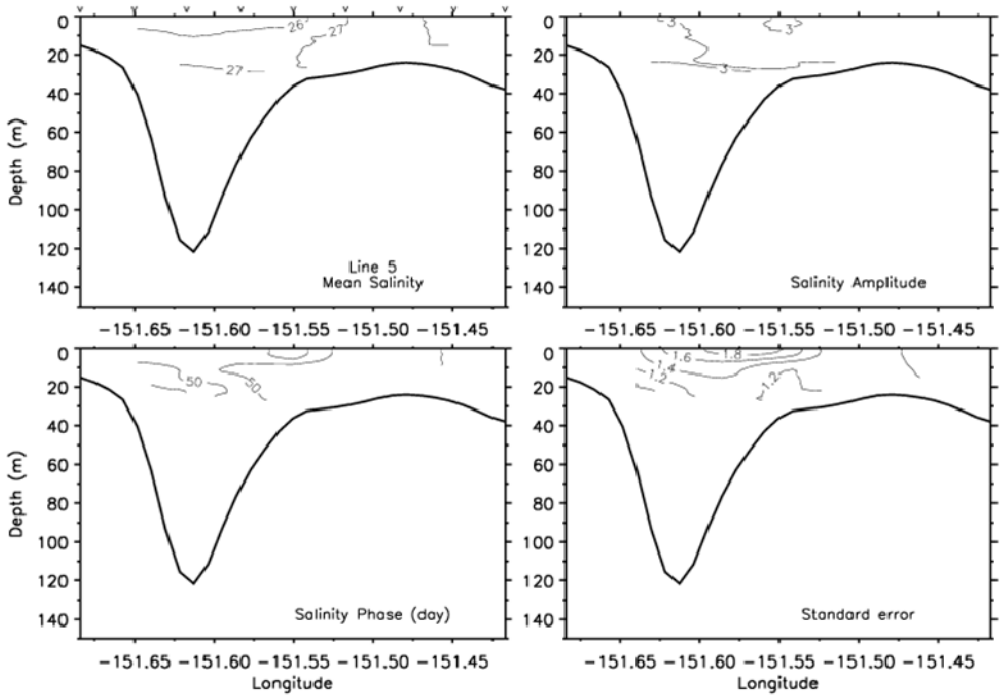

Figure 9. Fitted salinity data for line 4 is presented with the same order as figure 8.

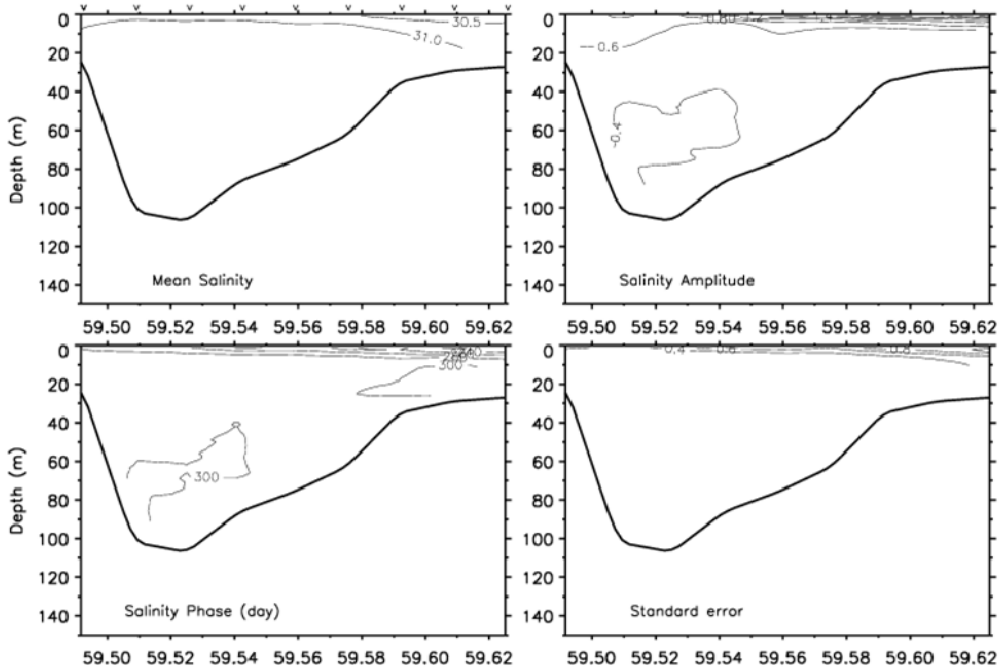

Figure 10. Fitted salinity data for line 3 is presented with the same order as figure 8.

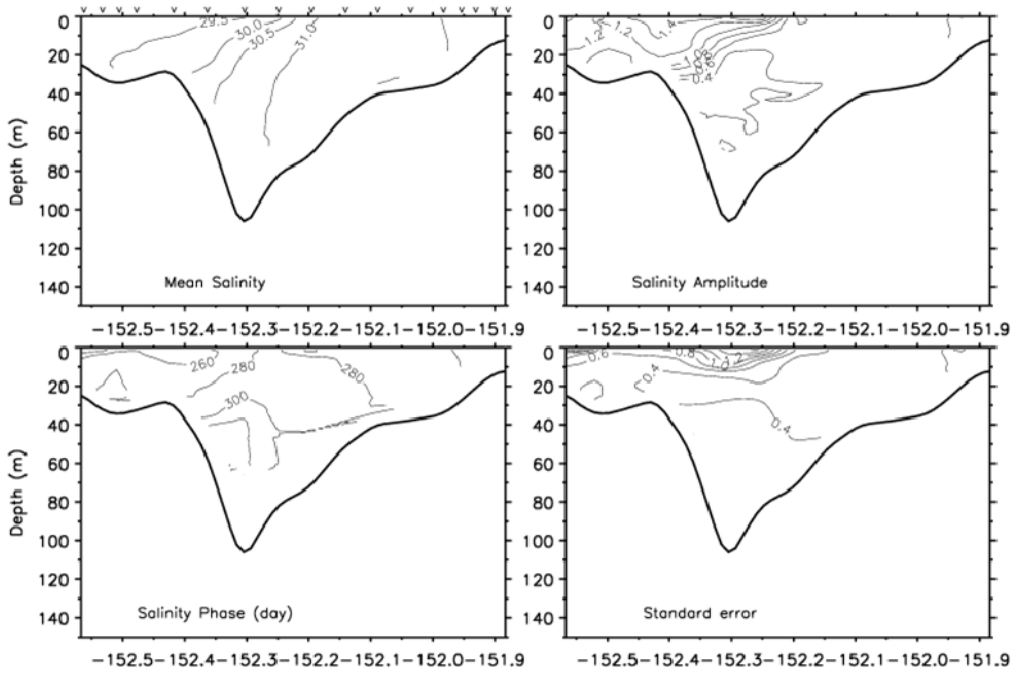

Figure 11. Fitted salinity data for line 2 is presented with the same order as figure 8.

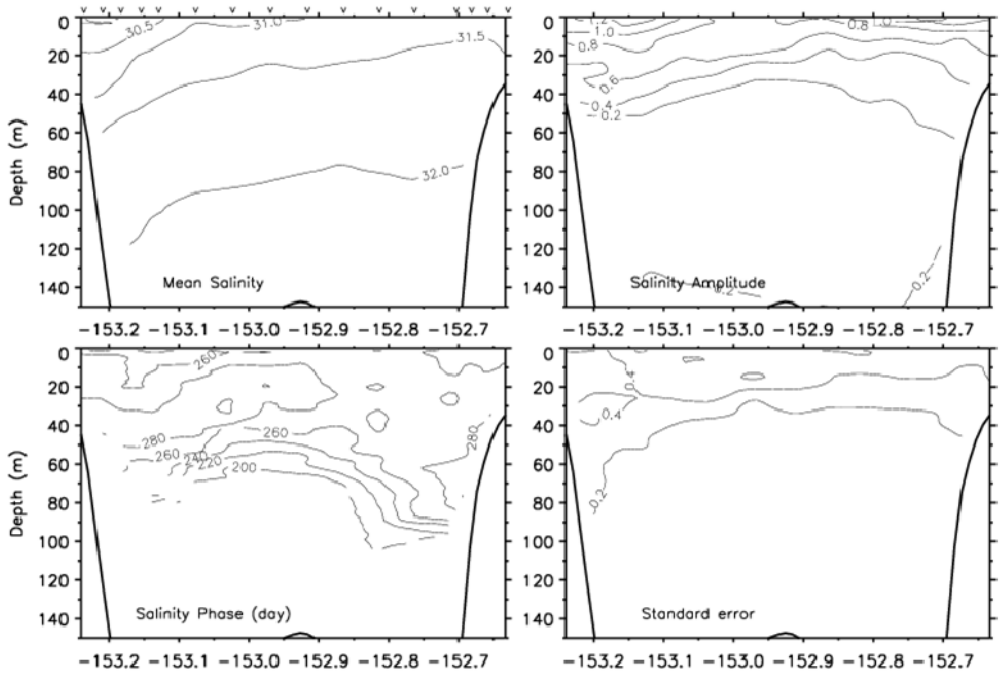

Figure 12. Fitted salinity data for line 1 is presented with the same order as figure 8.

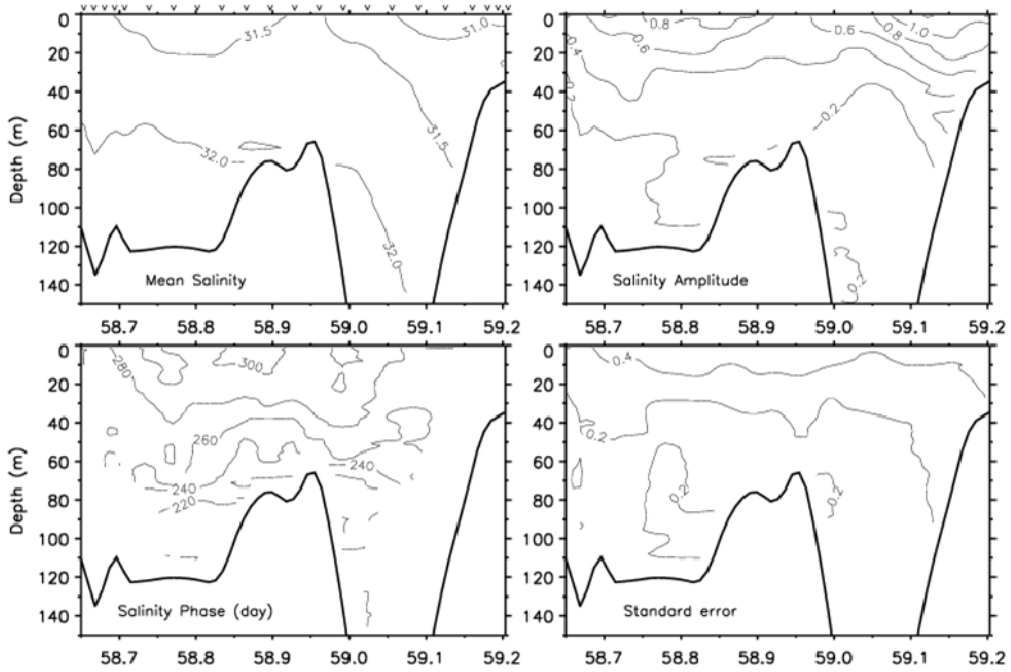

Mean conditions and seasonal variability of temperature

The seasonal cycles (mean, amplitude, phase, and standard error) of temperature along transect lines 1-5, as estimated using the least squares procedure, are summarized in Figures 13-17. Due to the large tidal range and shallow bathymetry of the upper Inlet, upper Inlet waters warm rapidly in late spring-early summer and cool rapidly during the autumn months. Because the lower Inlet waters are directly influenced by communication with northern Gulf of Alaska waters, lower Inlet temperatures are warmer in the mean and exhibit less seasonal variability than in the upper Inlet.

The lowest mean temperatures (~5-5.5°C) and the largest amplitude seasonal temperature signal (~8.5°C) within the study occur between the Forelands. The alert reader will note that the resulting least squares estimate of the temperature minimum is about –3°C. For the observed salinities such an ocean temperature is a physical impossibility and, as such, suggests that the limited number of surveys contributes to the unrealistic quantitative estimate. The associated phase plot indicates that the maximum temperature occurs in mid-August.

Mean temperatures along line 3 vary little, ranging from ~6.5°C on the west side of the line to ~7°C on the east side of the line. Amplitude of the seasonal signal, while less than that near the Forelands, is relatively large (~6°C) on the west side compared to the amplitude (~4°C) on the east side. The temperature maximum occurs in late August.

Mean temperatures along line 2 show more thermal stratification than is evident on lines 3 and 5. The coolest temperature (~6.5°C) occurs at the western side of the line within a few kilometers of the coast. Temperatures >7.5°C characterize the rest of the surface layer. The amplitude of the seasonal signal in the surface layer is ~6°C near the western side of the line and ~4.5°C over the remainder of the line. The amplitude falls to ~1°C at depths of 80-100 m. The temperature maximum in the upper 100 m of the water column occurs in late August-early September. Note that the standard error becomes comparable to the amplitude of the seasonal signal at depths below ~100 m. This is much deeper than the ~30 m threshold depth for salinity estimates. This difference likely reflects the comparative ease with which heat is transmitted through the water column compared to salt (mass).

The warmest mean temperature (~8°C) on line 1 occurs in association with ACC surface waters near the northern end of the line. The ventilation of the 7.5°C isotherm suggests enhanced tidal mixing. The amplitude of the seasonal temperature signal is ~4°C in the core of the ACC. The amplitude is less than 1°C near the bottom between Shuyak Island and the Barren Islands. The warmest temperatures occur in September.

Mean temperatures along line 4 range from ~6.5°C near the bottom to ~7.5°C near the surface. The amplitude of the seasonal temperature signal is <3.5°C over most of the water column and is ~4°C near the surface. Maximum temperatures near the surface occur in late August and in mid-September at depth.

Figure 13. The plots are the fitted mean temperature (top left), the temperature amplitude (top right), the day of the maximum temperature (lower left), and the standard error of the fit (lower right) for line 5.

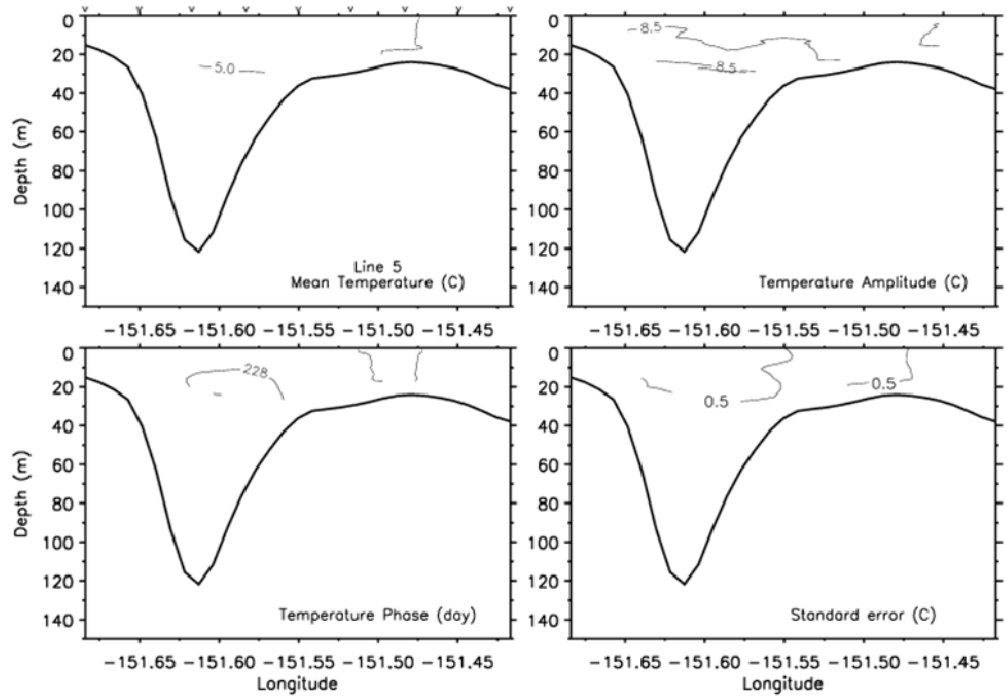

Figure 14. Fitted temperature data for line 4 is presented with the same order as figure 13.

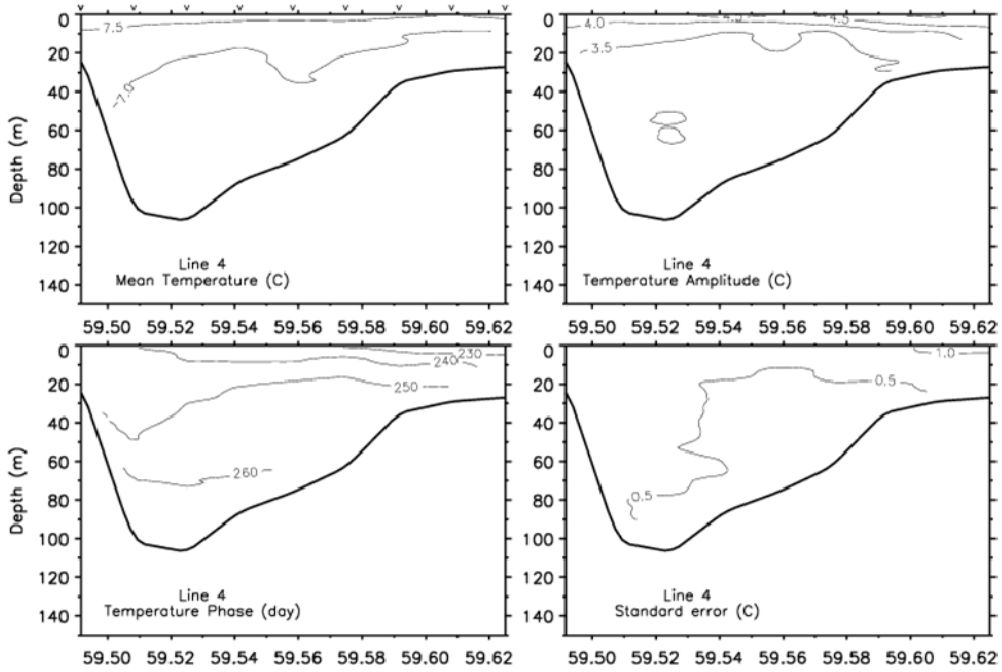

Figure 15. Fitted temperature data for line 3 is presented with the same order as figure 13.

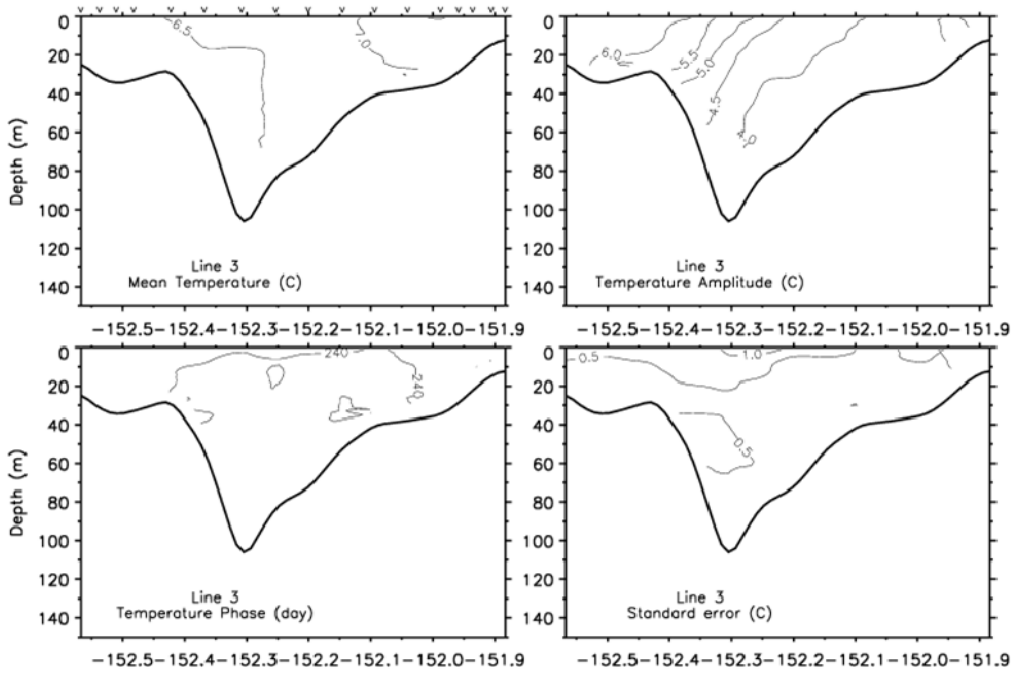

Figure 16. Fitted temperature data for line 2 is presented with the same order as figure 13.

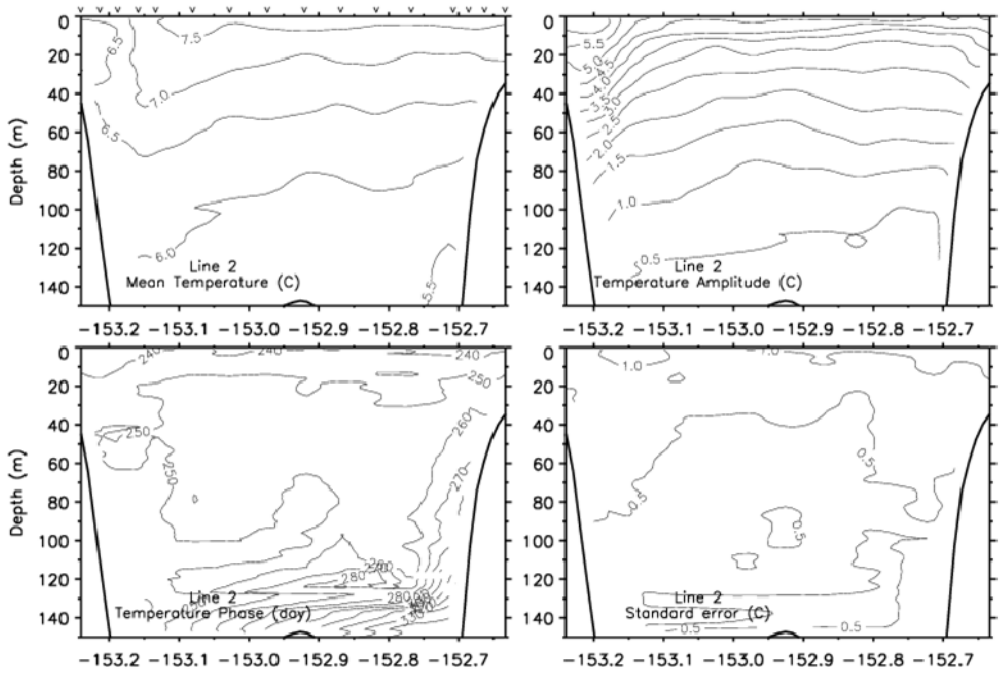

Figure 17. Fitted temperature data for line 1 is presented with the same order as figure 13.

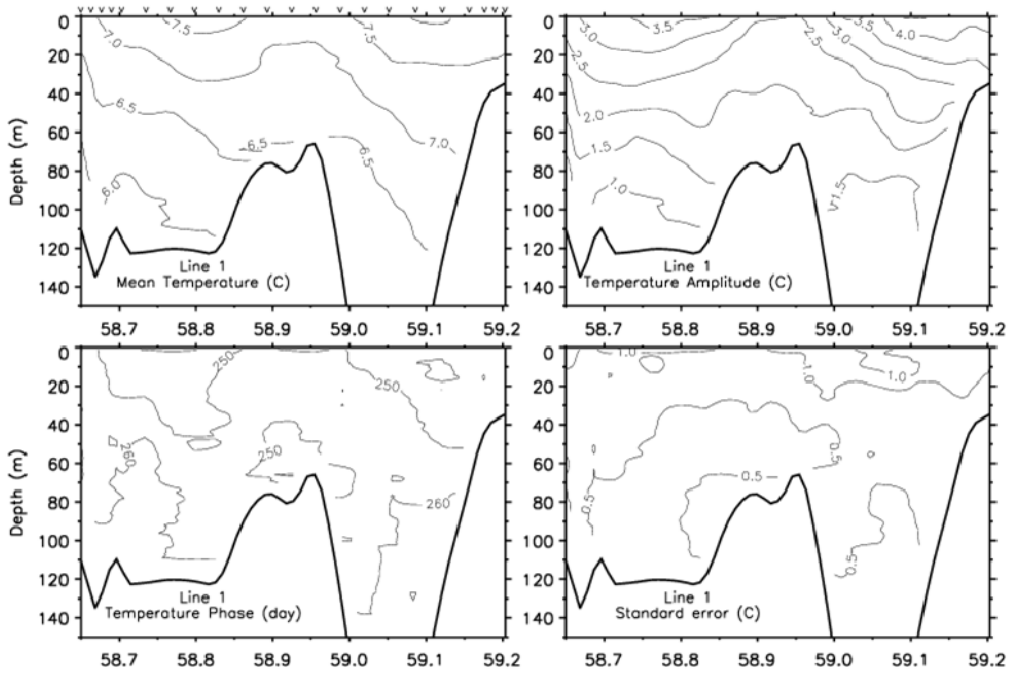

Salinity and temperature measurements representative of spring conditions (seasonally high salinity and low temperature) along lines 1-4 are shown in Figure 18. Corresponding measurements representative of late summer conditions (seasonally low salinity and high temperature) are shown in Figure 19. In the spring, the waters along each line are generally well mixed. In May, increased solar heating and freshwater inputs begin to promote stratification that intensifies through September.

Figure 18. April salinity (left column) and temperature (right column) contour plots are shown. Starting at the top the plots represent lines 1 through 4 in order.

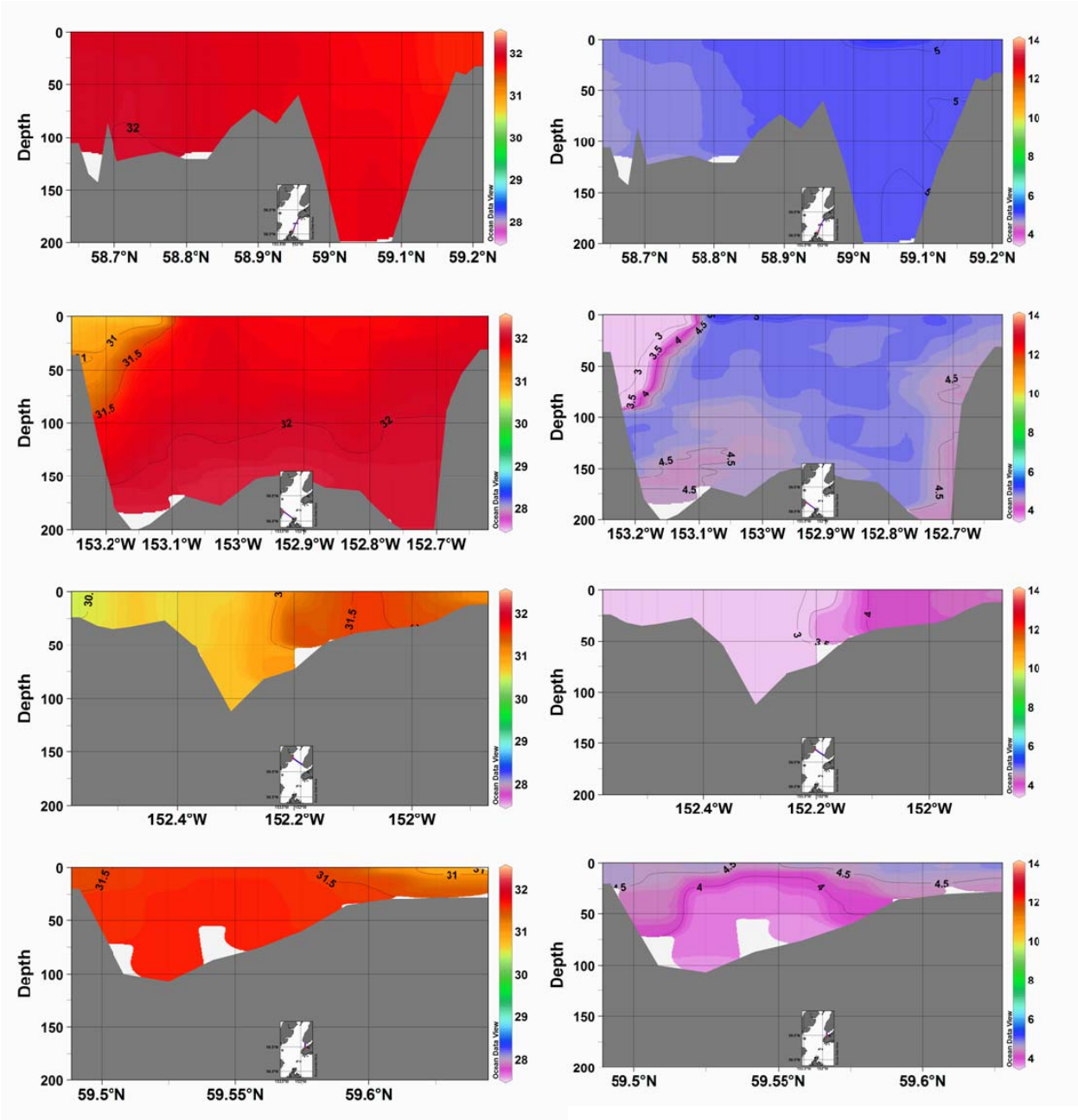

Figure 19. September salinity (left column) and temperature (right column) contour plots are shown. Starting at the top the plots represent lines 1 through 4 in order.

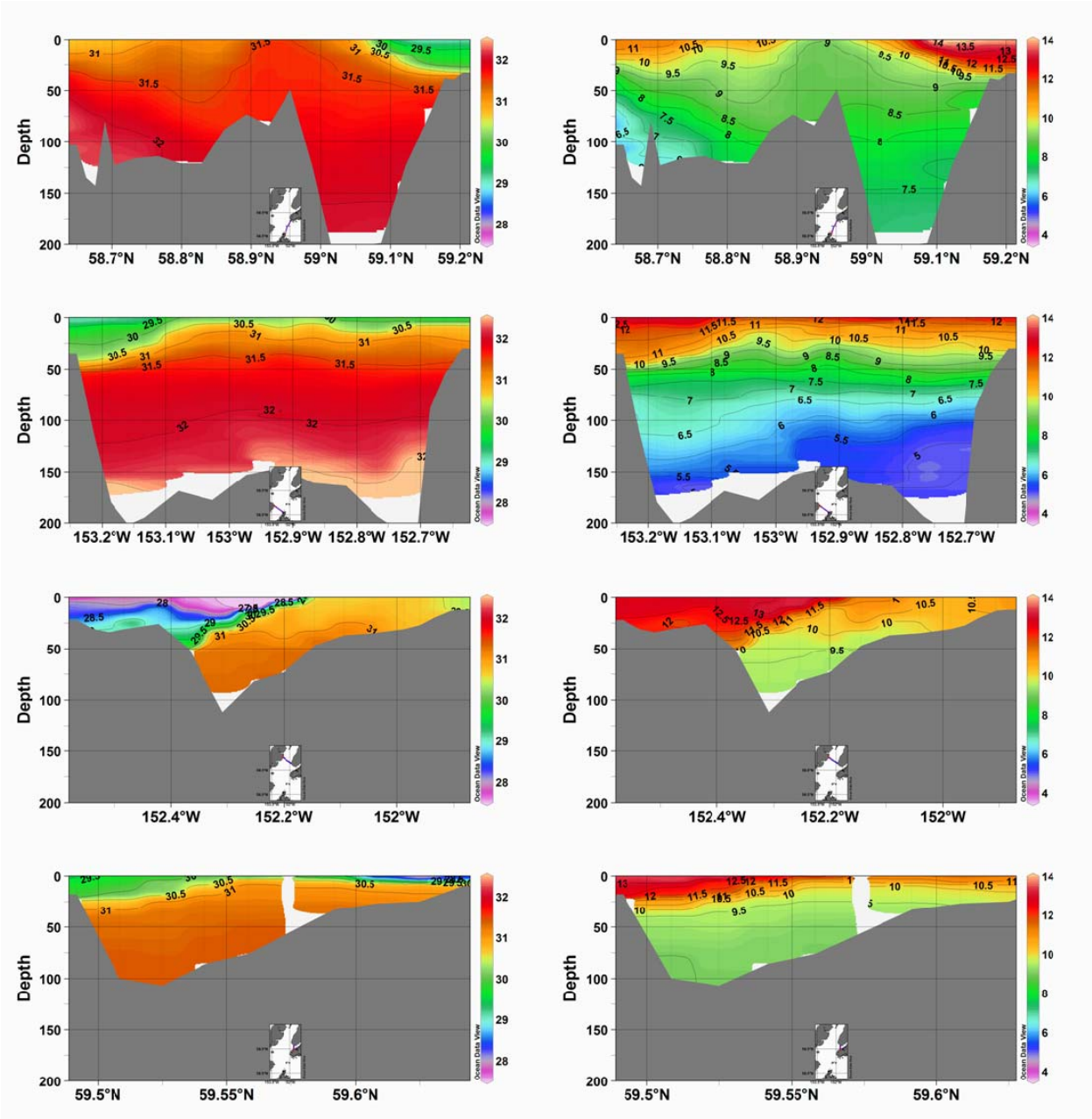

While seasonal cycles of temperature and salinity effect seasonal changes in the density field, spatial gradients in the density field result in baroclinic geostrophic currents. Geostrophic surface currents estimated from the density field show mean flows at a minimum in May and at maximum in September and October (Figures 20 and 21). In May, the estimated geostrophic currents are less than 0.2 m/s. They rise to over 1.0 m/s in the Western Cook Inlet (WCI) waters and 0.8 m/s in the ACC entering Cook Inlet. The strongest currents are in narrow bands in the fronts associated with the WCI waters and the ACC. Since freshwater inputs promote intensification of geostrophic currents, the seasonal evolution in freshwater transport is similar to the seasonal evolution of geostrophic currents (Figure 22). There is little

freshwater flowing through Kennedy Entrance from January to May. Freshwater transport then builds through October. Along line 3 there is a net southward freshwater transport in January that decreases until April, after which it increases through October. Southward freshwater transport through Shelikof Strait has a minimum in May and reaches a maximum in August.

Figure 20. Minimum geostrophic currents are observed in May. The scale arrow in the lower left represents 50 cm/s.

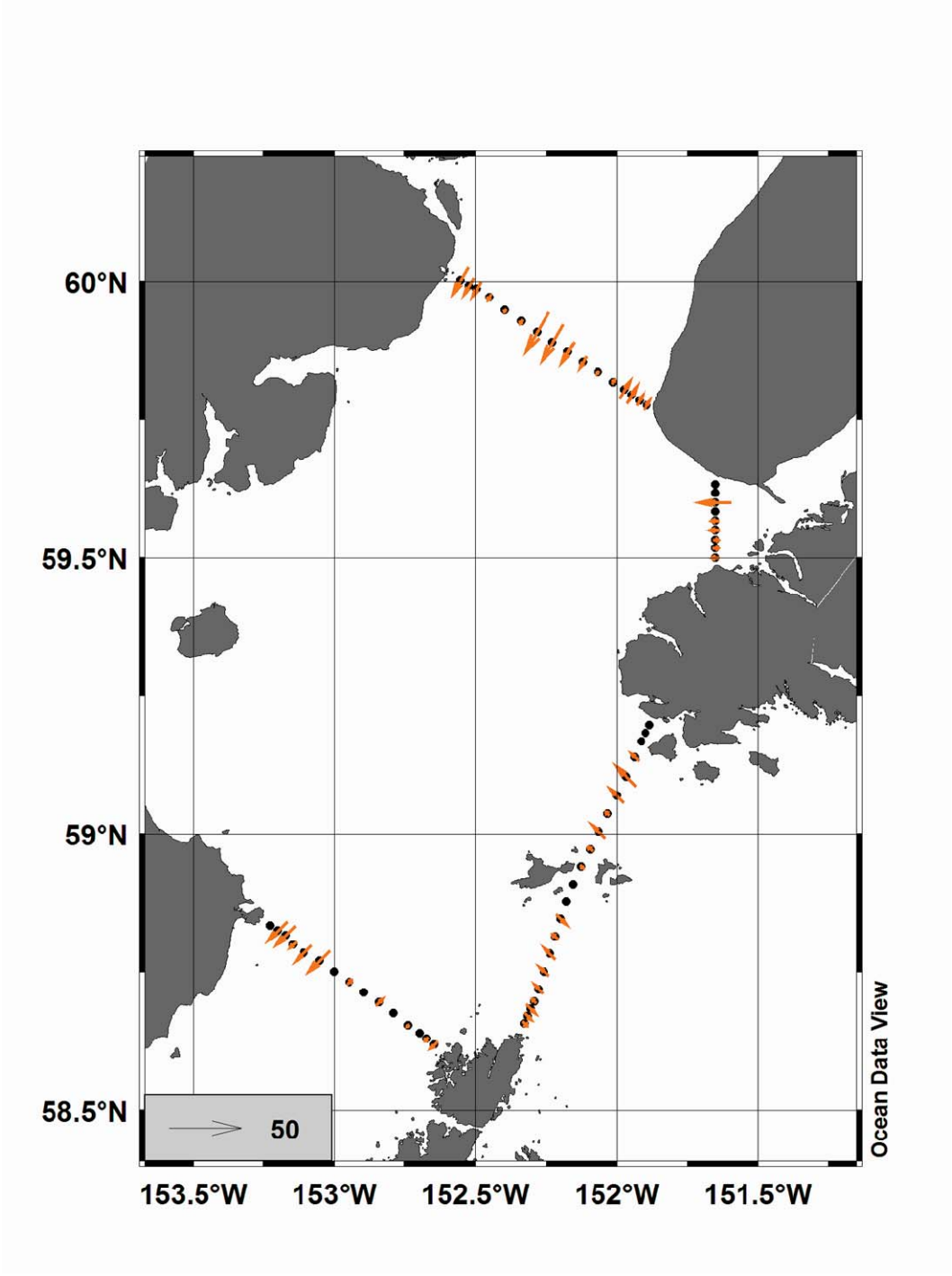

Figure 21. Maximum geostrophic currents are observed in September. The scale arrow in the lower left represents 50 cm/s.

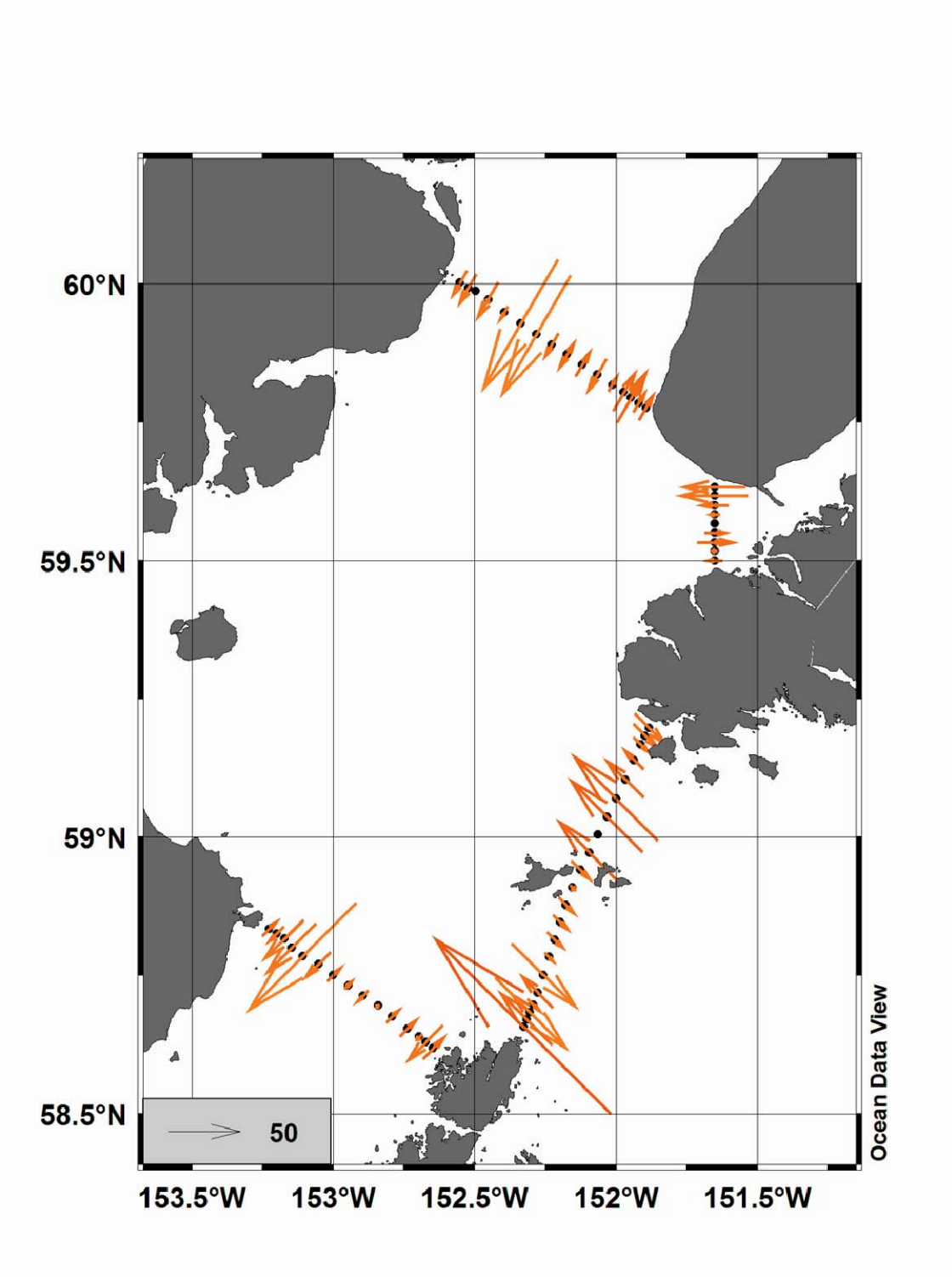

Figure 22. Freshwater transport by the geostrophic currents across lines 1 through 4 are provided. Negative transport is out of the box defined by the four lines. Line 1 is dotted, 2 is dashed, 3 is dash-dot, and 4 is three dots and a dash.

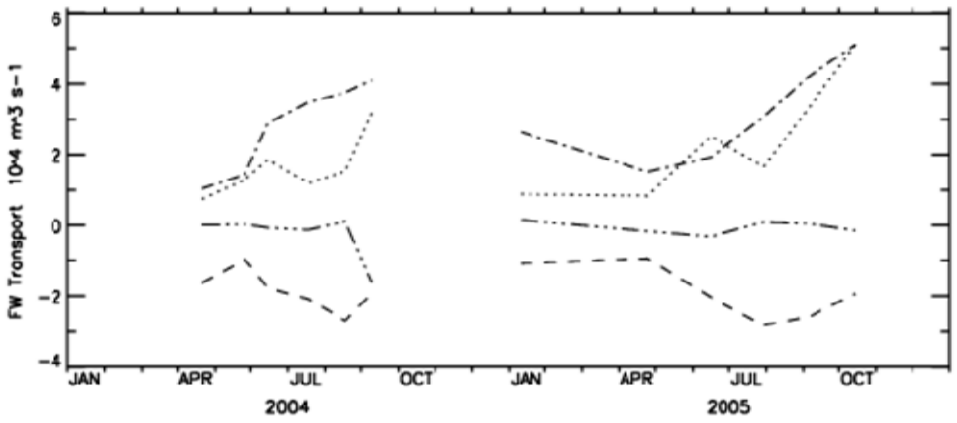

The seasonal patterns in oceanographic conditions are modified by forcing at shorter time scales. Cruises were conducted during spring and neap tides during the fall of 2006 to examine how circulation in lower Cook Inlet changed over the fortnightly tidal cycle. The three dates shown here are July 27th (spring tide), August 6th (neap tide), and August 13th (spring tide). Water levels in Seldovia during the sampling periods are provided in Figure 23.

Figure 23. Water levels in meters at Seldovia during the 2006 spring-neap tide measurement sequence are provided with the sampling period outline in blue.

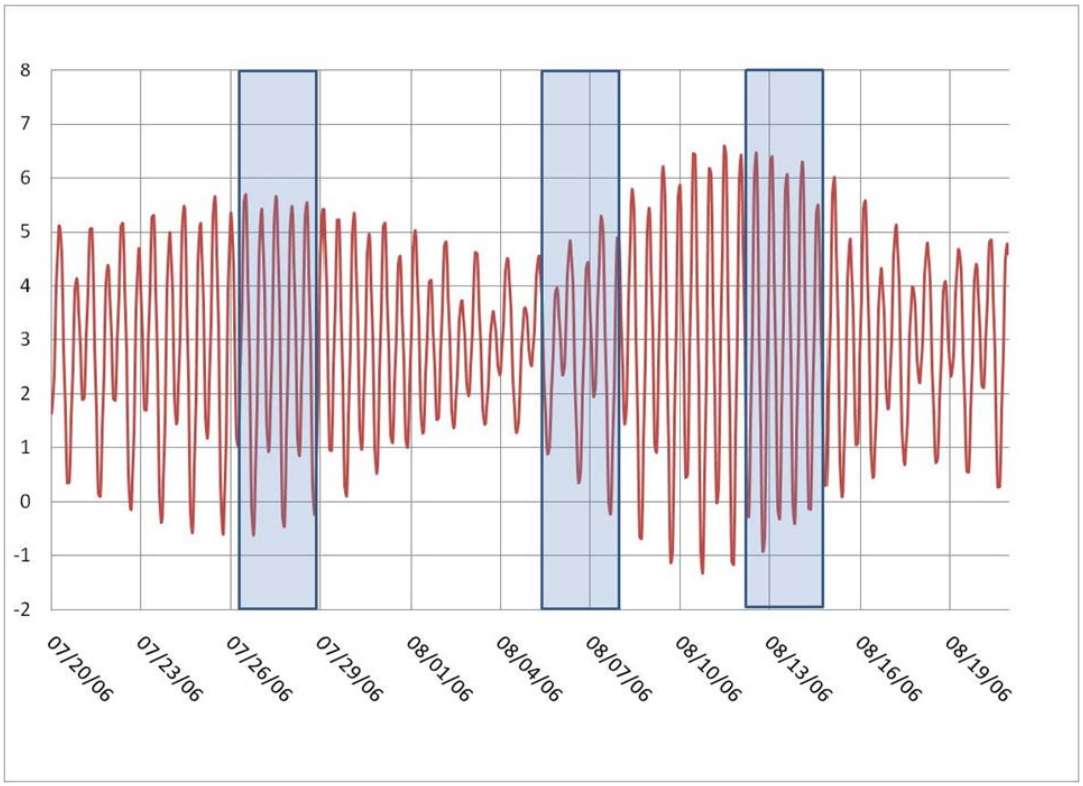

A few characteristics of the conditions along line 1 were observed to change. The ACC is evident during all three sampling periods (Figure 24), but the salinity decreases within the ACC as time progressed. During spring tides in Kennedy Entrance, more saline waters push onto the eastern shelf, altering the base of the ACC. The temperature of the deep water increases, and salinity decreases during spring tides. The temperature of the ACC was highest during the neap tide when mixing with deep water is minimized. Tidal mixing at the Barren Islands creates a colder, more saline water mass around the islands. The width of the cold water mass was greatest during spring tides. During the neap tide, a colder, saltier water mass is seen at the bottom of Stevenson Entrance. The temperature data suggests that this water mass spills into Kennedy Entrance around the Barren Islands.

Strong winds combined with the large spring tides made conditions too rough to sample in Shelikof Strait on the two spring tides of this sequence. Therefore, we were unable to observe changes in Shelikof Strait as a function of the strength of the tide.

Line 6 was placed directly across the mouth of Cook Inlet between Cape Adams in the east and Cape Douglas in the west. Line 6 had similarities to the patterns observed along line 1 (Figure 25) in that the salinity of the ACC decreased and the WCI salinity increased. At the same time, the bottom had an increasing presence of a colder, saltier water mass throughout the measurement sequence. It typically took about 30 hours from when we started sampling in Kennedy Entrance until we returned to Cape Adams along line 6. This temporal difference can help explain some of the differences observed along the eastern portions of lines 1 and 6.

We observed an increase in surface salinity during the spring tides along line 6. During spring tides, the core of the ACC waters remains less than 50 m deep, whereas during neap tide the ACC can be observed down to 100m. The deep portion also detached from the shore. During the spring tide there is a salt wedge in the center of Cook Inlet that separates the freshwater flowing into and out of Cook Inlet. On the neap tide the freshwater plume is observed across the entire mouth of Cook Inlet.

More dramatic changes between the spring and neap tide conditions can be seen a little further into Cook Inlet along line 7 (Magnet Rock to Augustine Island, Figure 26). A freshening of the surface waters is observed along the western boundary. The greatest difference between the spring and neap tides occurs in the center of the transect and along the bottom. On a spring tide there are two colder, more saline parcels of water along the bottom separated by a warmer, fresher water mass in the center. The salinity of the western tongue of salty water decreased through the final sampling in September. During the neap tide the cold-salty water extends from the bottom to nearly the surface in the center of the transect.

Further north along line 3 (Anchor Point to Tuxedni Bay) the most obvious difference between the spring and neap tide conditions is the extent of WCI water (Figure 27). During a neap tide the typical surface salinities are <28 PSU with strong stratification. Fresher water is observed along the eastern side of the channel. During the spring tide the salinity of the WCI water is approximately 30 PSU and the stratification is reduced.

Other sources of data are useful in observing the effects of the spring-neap cycle on the water properties of Cook Inlet. The Alaska Department of Fish and Game has been monitoring oceanographic conditions in the channel portion of line 3 for several years. They make daily transects, and some of the salinity data from 2005 can be seen in Figure 28. During the neap tides (1-5, 15-19, 29-31 July), stratification increases and surface salinities decrease in the WCI waters. As the tidal amplitude increases into the spring phase (7-13 and 21-27 July), the WCI becomes mixed throughout the water column resulting in a thicker, more saline water mass. The amplitude of the fortnightly salinity signal of the WCI water mass is ~1.5.

Figure 24. Salinity contours along line 1 are displayed in the left panel and temperature in the right. The data in the panels are from July 27 (spring tide), August 6 (neap tide) and August 13 (spring tide) as viewed from top to bottom.

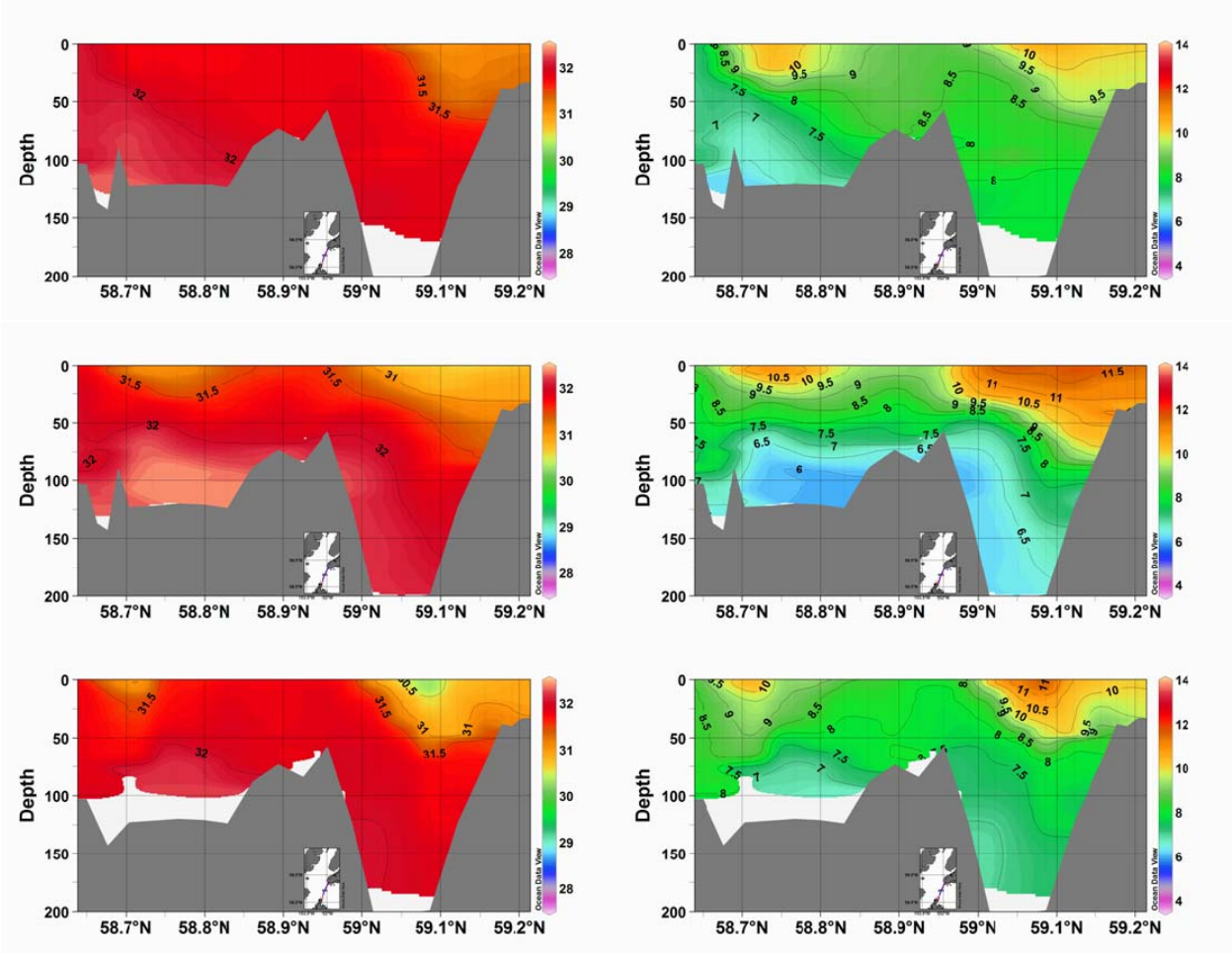

Figure 25. Salinity contours along line 6 (Cape Adams to Cape Douglas) are displayed in the left panel and temperature in the right. The data in the panels are from July 27, August 6 and August 13 as viewed from top to bottom.

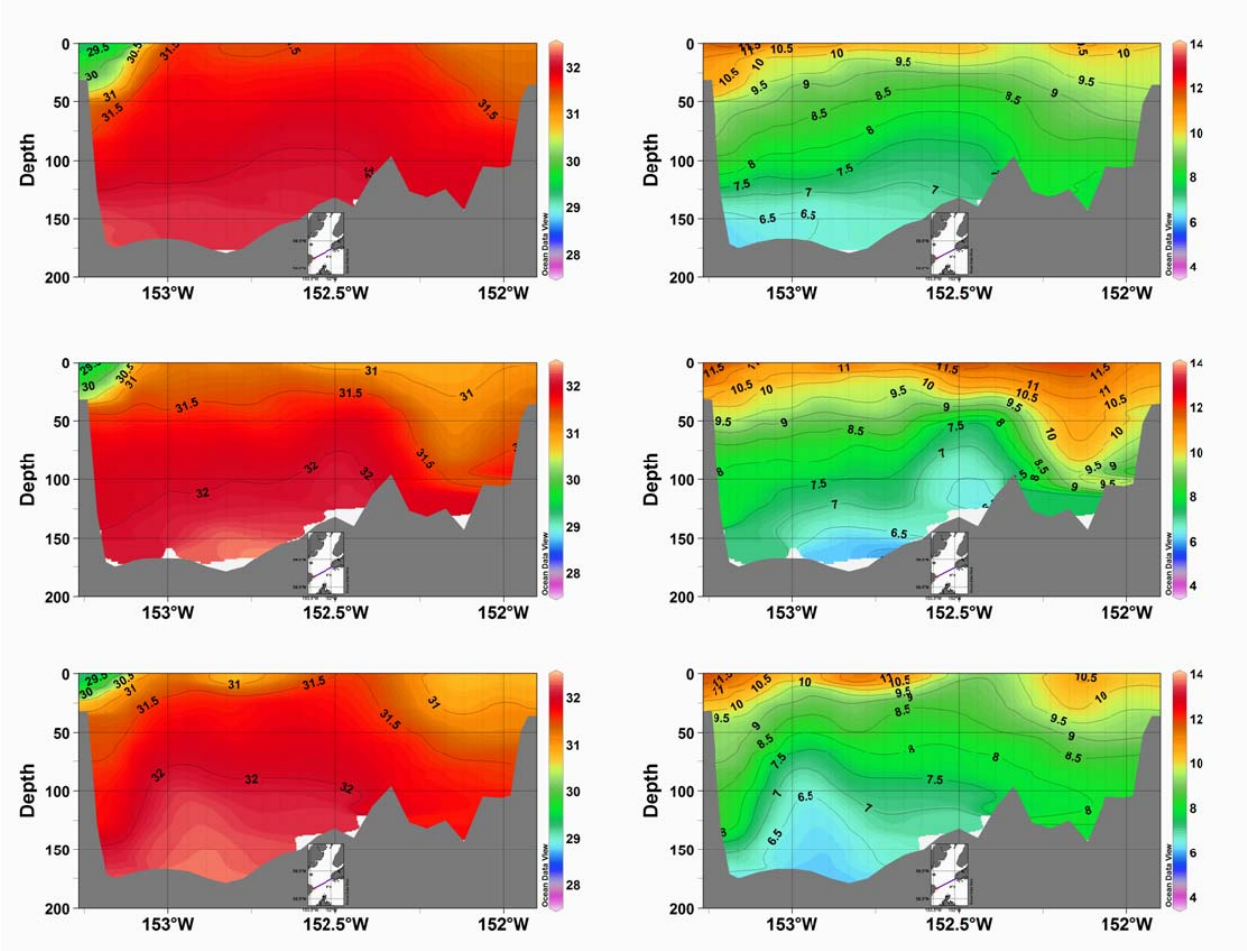

Figure 26. Salinity contours along line 7 (Magnet Rock to Mt. Augustine) are displayed in the left panel and temperature in the right. The data in the panels are from July 27, August 6 and August 13 as viewed from top to bottom.

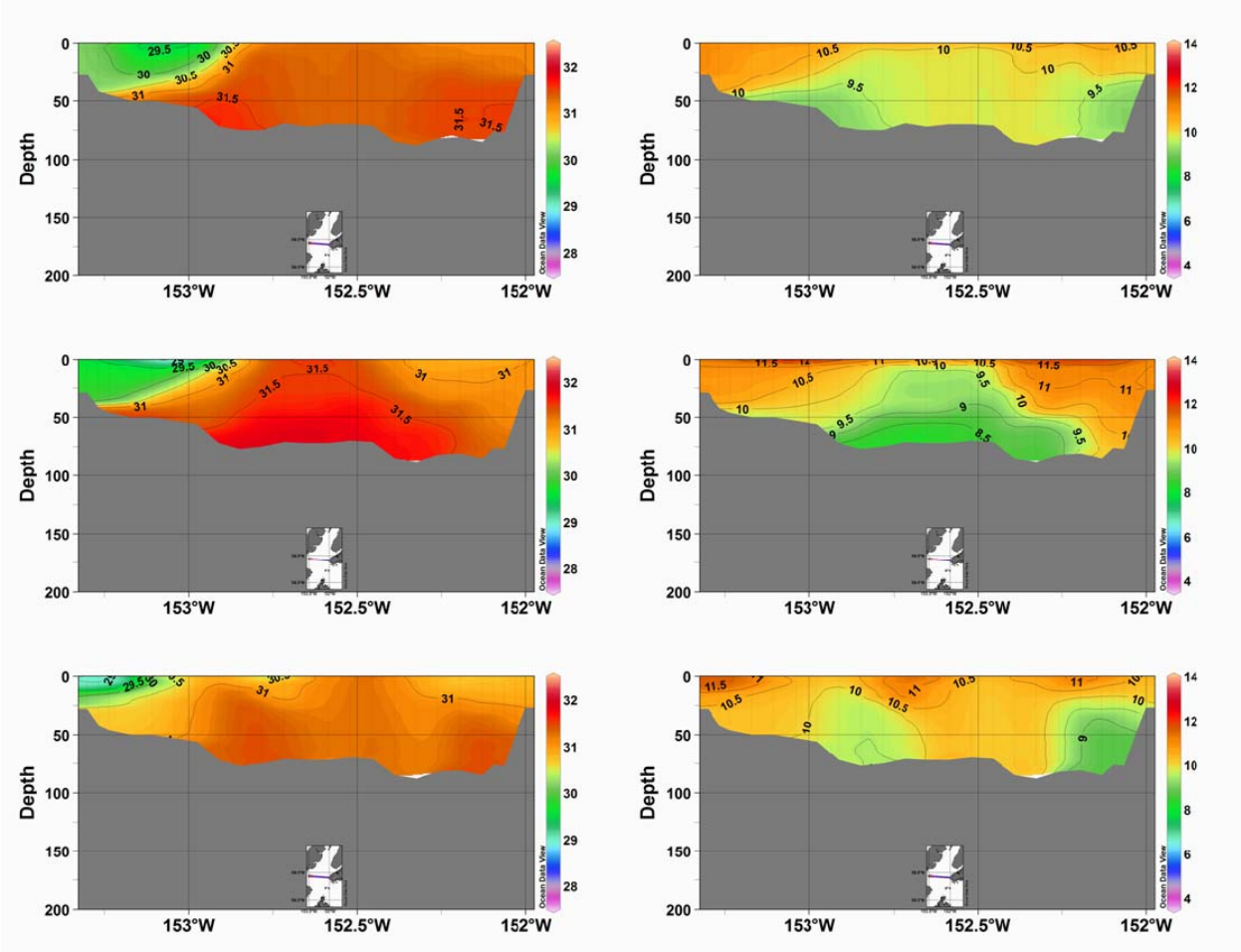

Figure 27. Salinity contours along line 3 are displayed in the left panel and temperature in the right. The data in the panels are from July 27, August 6 and August 13 as viewed from top to bottom.

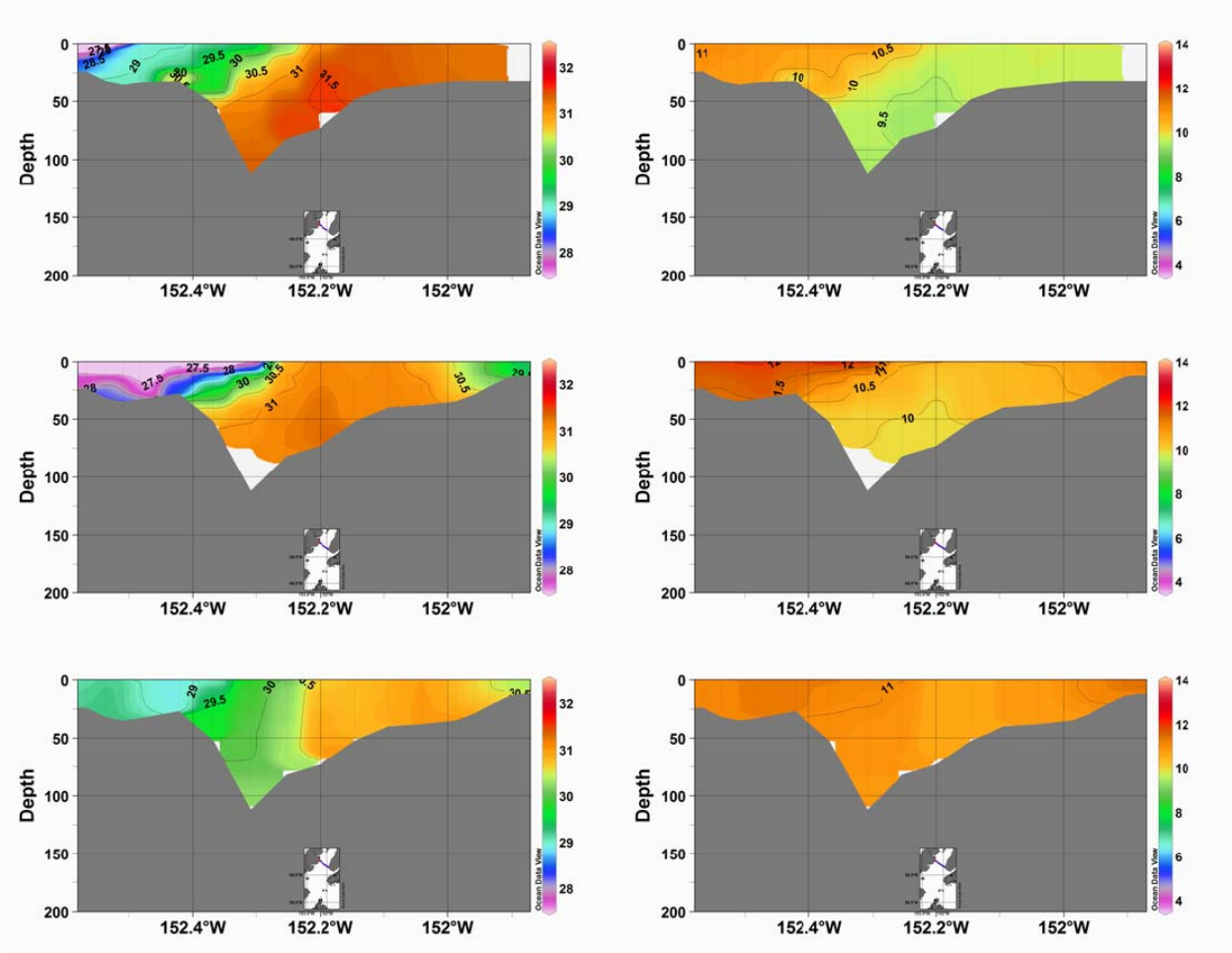

Figure 28. Salinity contours measured during 2005 by the Alaska Department of Fish and Game Offshore Test Fisheries program. The number in the corner is the day in July that the data was collected.

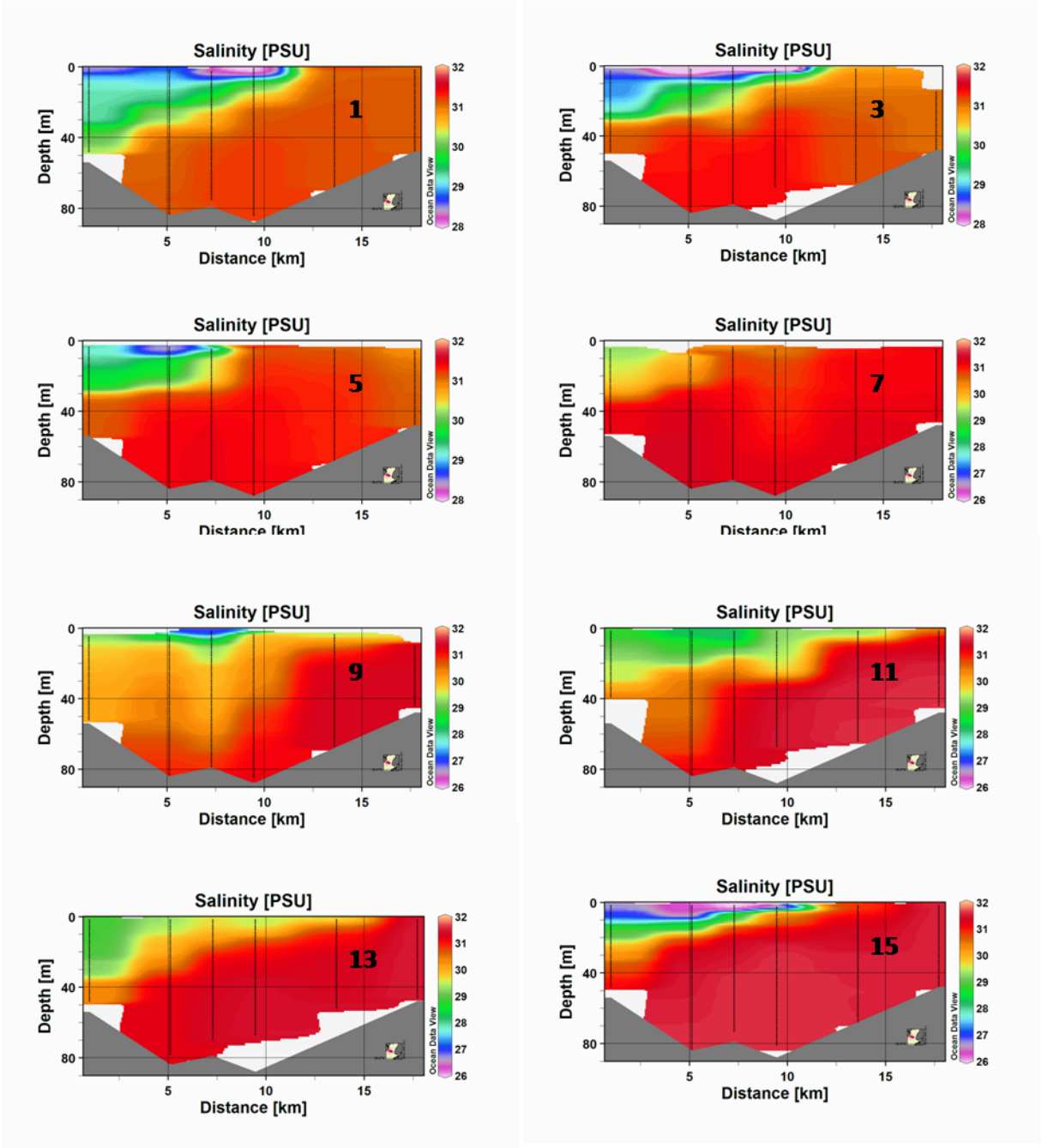

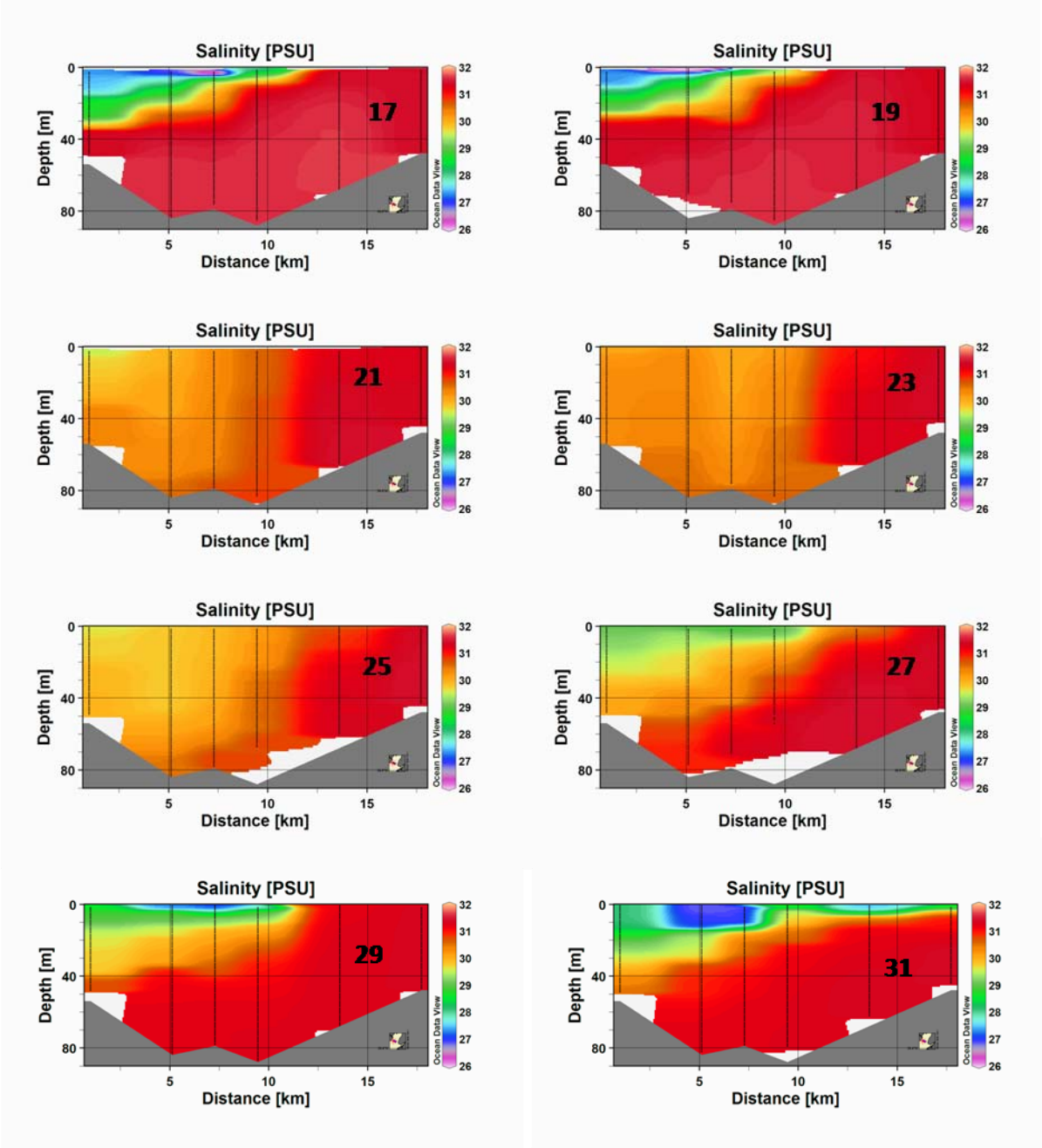

Another illustration of fortnightly changes in water properties is provided by data from the mooring deployed in August 2006 along the eastern shelf of Kennedy Entrance (Figure 29). During spring tides the salinity along the bottom of the shelf increases consistent with that presented in Figure 24. During neap tides, salinity decreases as the strength of the ACC increases. The amplitude of the fortnightly salinity signal is ~1 at the mooring location. Large fluctuations in salinity are also observed during the semidiurnal tide cycle (Figure 30). A representative amplitude of the semidiurnal salinity signal is about 0.5. Although not shown here, a representative amplitude of the near surface semidiurnal salinity signal at the XTO platform was ~1.2. At both mooring sites, the amplitudes of the semidiurnal salinity signals were somewhat larger during spring tides than during neap tides.

Figure 29. Salinity and depth data collected by a mooring on the eastern shelf of Kennedy Entrance is presented.

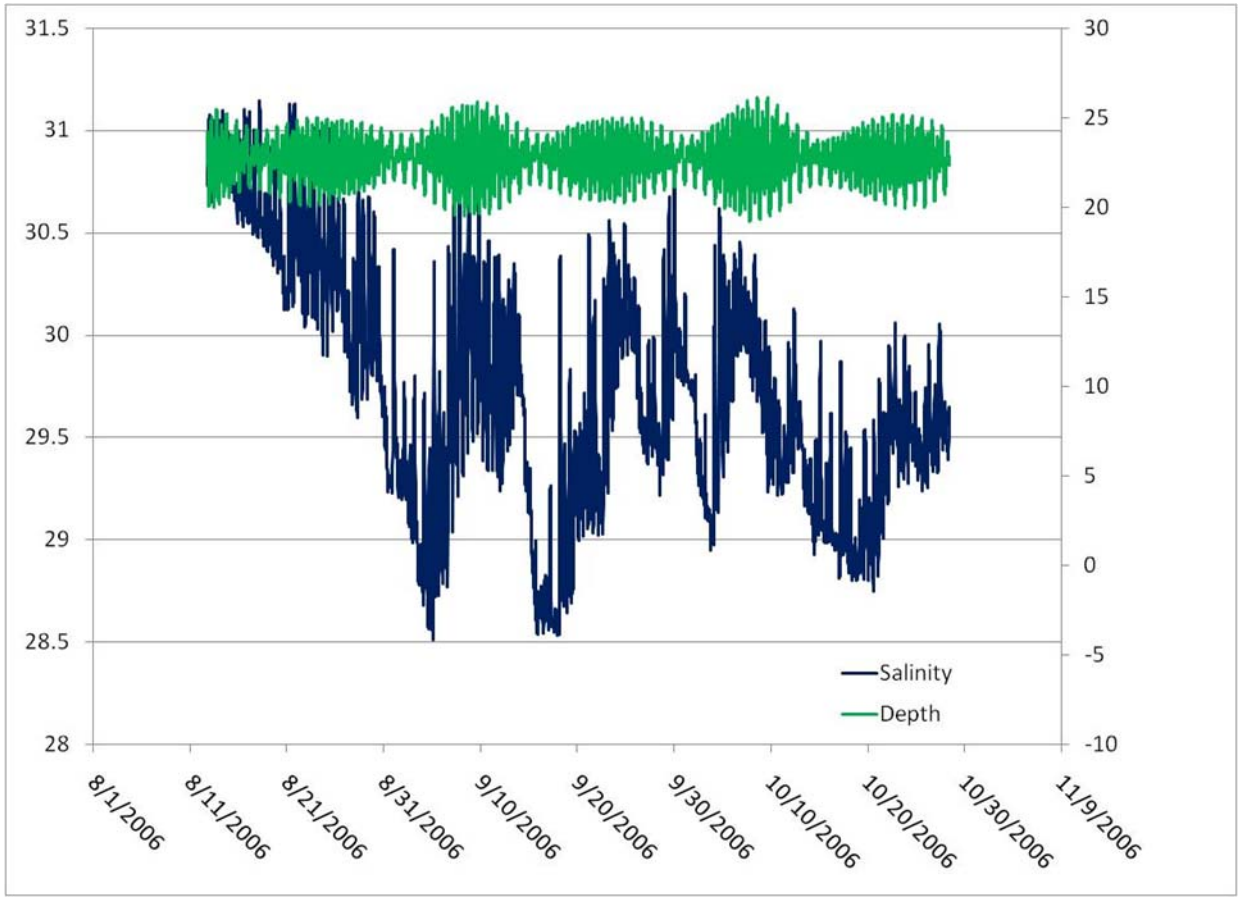

Figure 30. A short segment of the data presented in figure 29 is presented to show the fluctuations in salinity with tide stage.

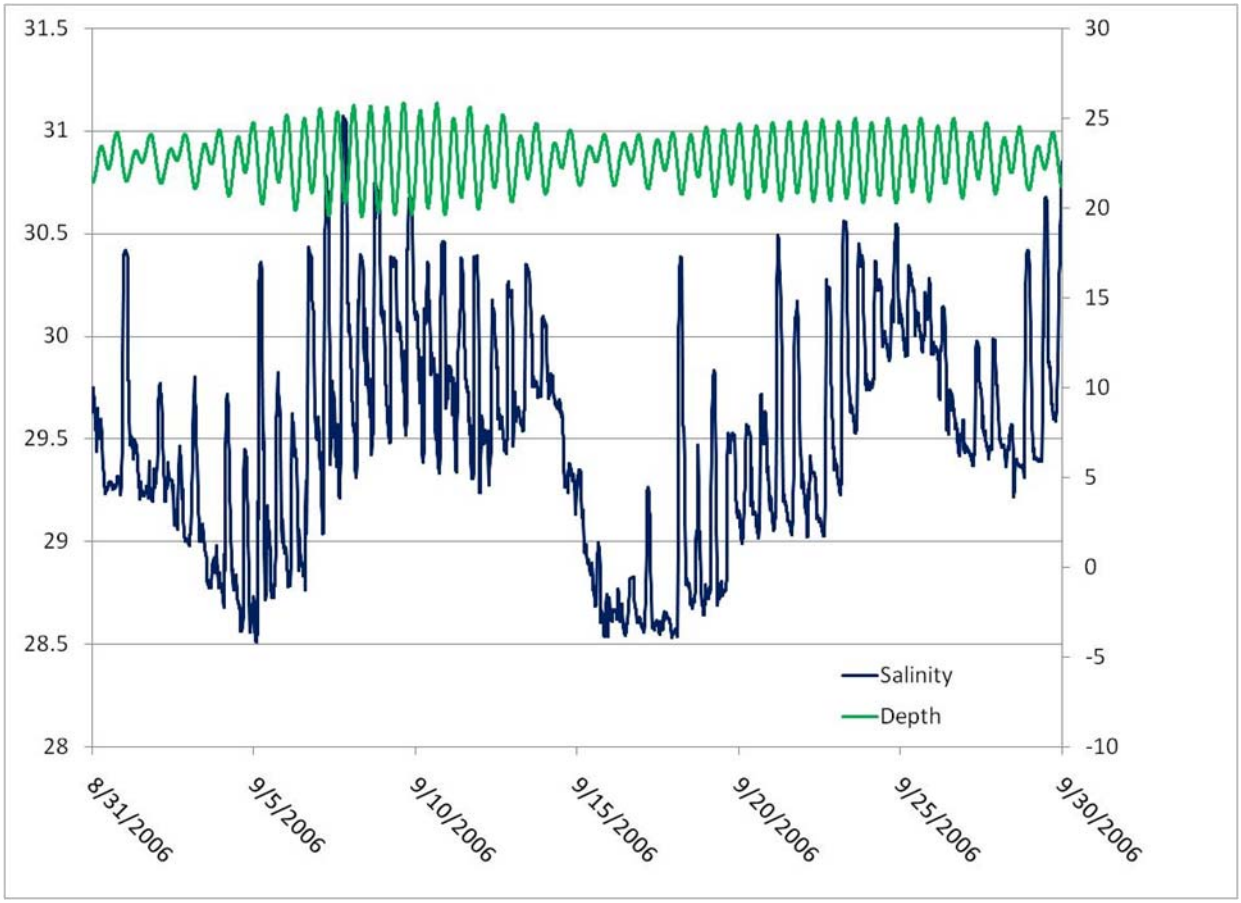

DISCUSSION

Variability in oceanographic conditions occurs at time scales of minutes to decades. The tide station temperature data records show the Pacific Decadal Oscillation and shorter term climatic shifts that are on the order of five to eight years in duration. Seasonally there is a fairly consistent pattern in the oceanographic temperature. Starting in March the water begins to warm at a fairly constant pace until July. There is a small peak in temperature in August, but the temperature is fairly steady between July and September. Beginning in October there is a rapid decrease until December. The temperatures then remain low through March.

Surface temperatures on the western side of Cook Inlet were observed to go through the largest temperature fluctuations. Surface waters along the west side of Cook Inlet originate in the upper Inlet where the very shallow depths promote efficient cooling in winter and heating in summer. While the western side of Cook Inlet had the most extreme temperature changes, the seasonal cycle was observed throughout lower Cook Inlet waters. The one exception to this pattern occurred in the deepest waters of Shelikof Strait. In the bottom of Shelikof Strait a cold-saline water mass moved in during the summers causing some of the lowest temperatures at the bottom to occur during the summer. This intrusion of more saline waters is consistent with the salinity signal observed along the Gulf of Alaska line as described by Royer (2005).

Seasonal changes in the freshwater inputs drive seasonal changes to the salinity field of the Cook Inlet region. There are two principal sources of freshwater to the study area, river discharge into upper Cook Inlet and ACC transport into lower Cook Inlet. A typical seasonal river discharge profile somewhat resembles a step function. Following the winter discharge minimum, river discharge increases by more than an order of magnitude during May. Discharge remains high through the summer, though variable, and decreases from late September through November. While freshwater is carried into lower Cook Inlet throughout the year by the ACC, the freshwater signal varies with seasonal changes in coastal precipitation and wind mixing. The resulting ACC salinity minimum occurs in late September-early October; about a month later than the salinity minimum occurs in central Cook Inlet

The seasonal variability in temperature and salinity sets up the hydrographic conditions that drive the currents in lower Cook Inlet. There are several potential problems with the geostrophic currents estimated from the hydrographic measurements. These include: strength of the tidal currents may inhibit the ability to reach geostrophic balance, the spacing between stations being short, current estimates are only for the portion perpendicular to the transect line, and assuming a level of no motion forcing the solution to provide only the baroclinic portion of the current. The errors in the estimated currents are then reflected in the freshwater (FW) transport estimates, which show a net positive FW transport into the survey area (Figure 22), which implies an increase in mass within the region. While these calculated currents have their limitations, when combined with other sources of information we can begin to provide a better picture of circulation in the region.

It is possible to make some inferences about the flow in lower Cook Inlet using the freshwater content estimates. The freshwater content observed along lines 6 and 7 was greater than the amount flowing through Kennedy Entrance and south past line 3. The amount of freshwater was greatest along line 6 due to the transect line being aligned with the direction of flow, implying that the ACC is crossing Cook Inlet near this line.

After subtracting the southward flowing freshwater observed on line 3, the freshwater content along line 7 was typically around 65% of that seen along line 6. This result was independent of the spring-neap tide cycle. Only on the neap cycle is there a clear pulse of ACC water traveling northward past line 7 and into Kachemak Bay. During spring tides, wedges of saltier water are observed near the bottom on each side of

the Inlet with a fresher water section between them. This fresher section is most likely the northern edge of the ACC. Anecdotal evidence for this inference was the significant amount of debris, particularly fucus and free-floating bull kelp, which signified the presence of a front.

The fresher water flowing out of lower Cook Inlet appears to be restricted to a band approximately 5 -9 km wide as it passes Cape Douglas (Figures 1 and 25). This narrow outflow contains most of the freshwater flowing south along the west side of Cook Inlet and the ACC waters flowing into Cook Inlet. In every one of our observations along line 6 the cross-sectional area of the freshwater band flowing out of Cook was smaller than the cross-sectional area of the ACC flowing into Cook Inlet at Cape Adams. For example, in Figure 25, the area of water entering with salinity less than 31.5 PSU is three times the area of equivalent salinity exiting Cook Inlet. This may be in part due to a stretching of the apparent area of the ACC caused by the transect line being at an angle to the direction of flow. A slightly smaller area of the ACC is observed along line 1, which has approximately the same starting location, but cuts across the ACC at a different angle. Even this smaller area observed along line 1 is double that seen passing Cape Douglas in Figure 25, and the water flowing pass Cape Douglas includes the ACC and WCI waters. This implies that the outflow past Cape Douglas must be much more rapid than the inflow in order to conserve mass. However, the geostrophic baroclinic current estimates don't reflect the existence of an intensified current along the western side of Cook Inlet. As a consequence, the baroclinic freshwater transports into and out of the lower Inlet do not sum to zero.

Mixing of ACC, WCI, and other Cook Inlet waters can be limited by the spring-neap tidal cycle. Figure 31 shows the WCI water cocooned within the ACC waters as they both flow into Shelikof Strait. A near-surface (< 15 m) lower salinity lens of WCI water is imbedded in a slightly higher salinity lens of ACC water at the northern end of Shelikof Strait. The origins of the two water masses are more evident in the temperature data where the imbedded lower-salinity water is at a colder temperature than the ACC water flowing into the lower Inlet through Kennedy Entrance and out through Shelikof Strait. We speculate that this phenomenon occurs only during periods of weak tidal mixing (neap tide) and high freshwater input.

Further into Cook Inlet, there is also evidence that tidal mixing may block the exchange of waters between areas. The temperature-salinity properties of the deep water in Kachemak Bay are not consistent with the properties of water flowing into Cook Inlet through Kennedy Entrance (Figure 32). We hypothesize that, during spring when the stratification is relatively weak and more conducive to the mixing of the water column, saltier waters form at the confluence of Cook Inlet and Kachemak Bay, even during the neap tide. This would restrict exchange of water between Kachemak Bay and Cook Inlet, which would account for the differences in the temperature-salinity characteristics between the two water bodies. As stratification increases during the summer months, the blocking water only forms during spring tides when tidal mixing is relatively strong. During neap tides when tidal mixing is weak, exchange between Kachemak Bay and Cook Inlet is enhanced.

The mixing of the colder-saltier water is also evident in the sea-surface temperature imagery (Figure 33) and ocean color imagery (Figure 34). This colder water is bounded on the west by the freshwater flowing down Cook Inlet, to the east by warmer water in Kachemak Bay, and to the south by the ACC. Fresher water to the west and east suggests that the colder water will follow a cyclonic (counter-clockwise) path.

Figure 31. Salinity contours along lines 1 and 2 are provided in the top panel and temperature is in the lower panel. The data presented is from October 2005 and shows the WCI water imbedded in the ACC as it passes into Shelikof Strait.

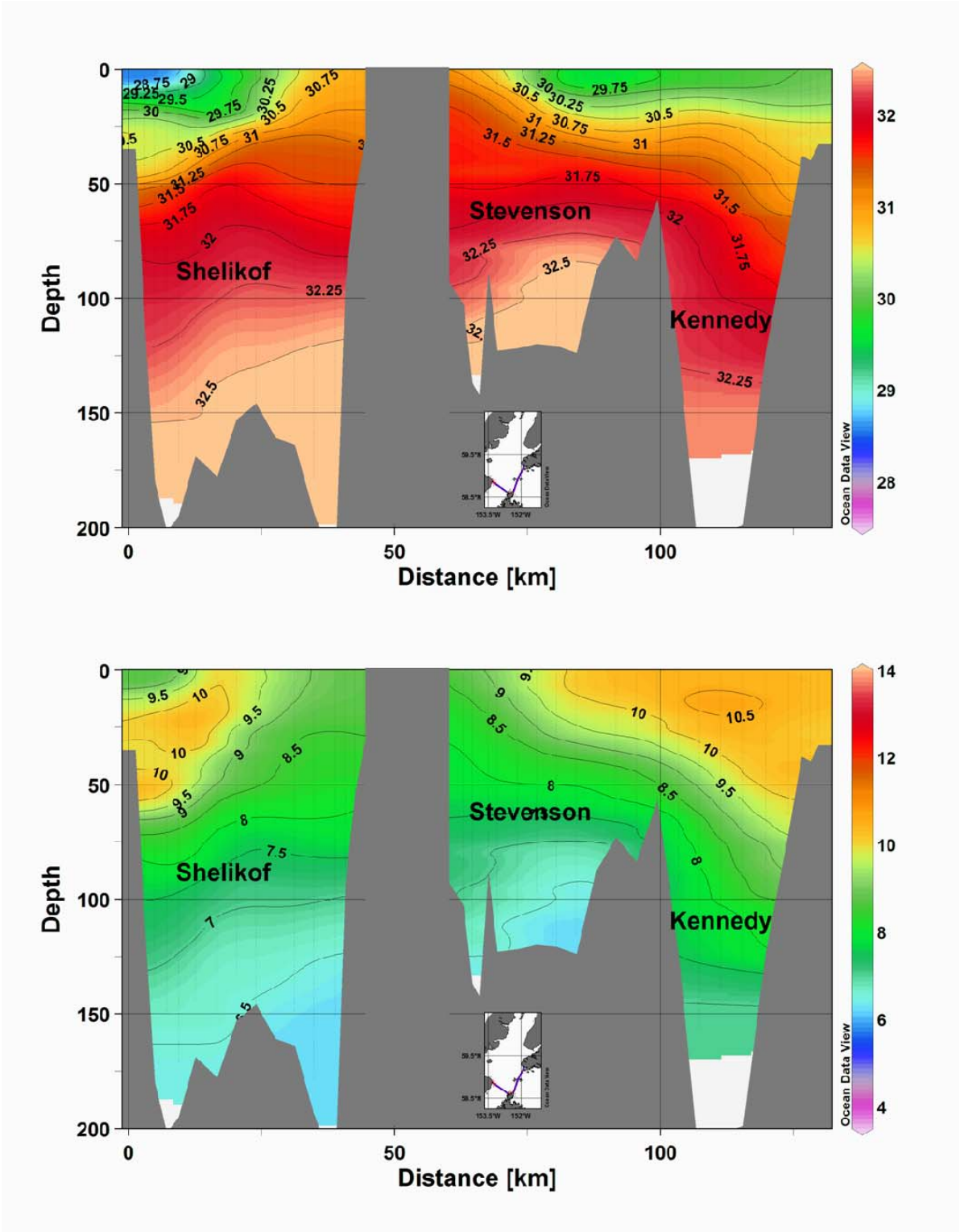

Figure 32. Temperature-salinity plots for April along line 1 (Kennedy), line 2 (Shelikof), line 3 (Anchor), line 4 (Barabara) showing that line 4 has a different characteristic than the other Cook Inlet waters.

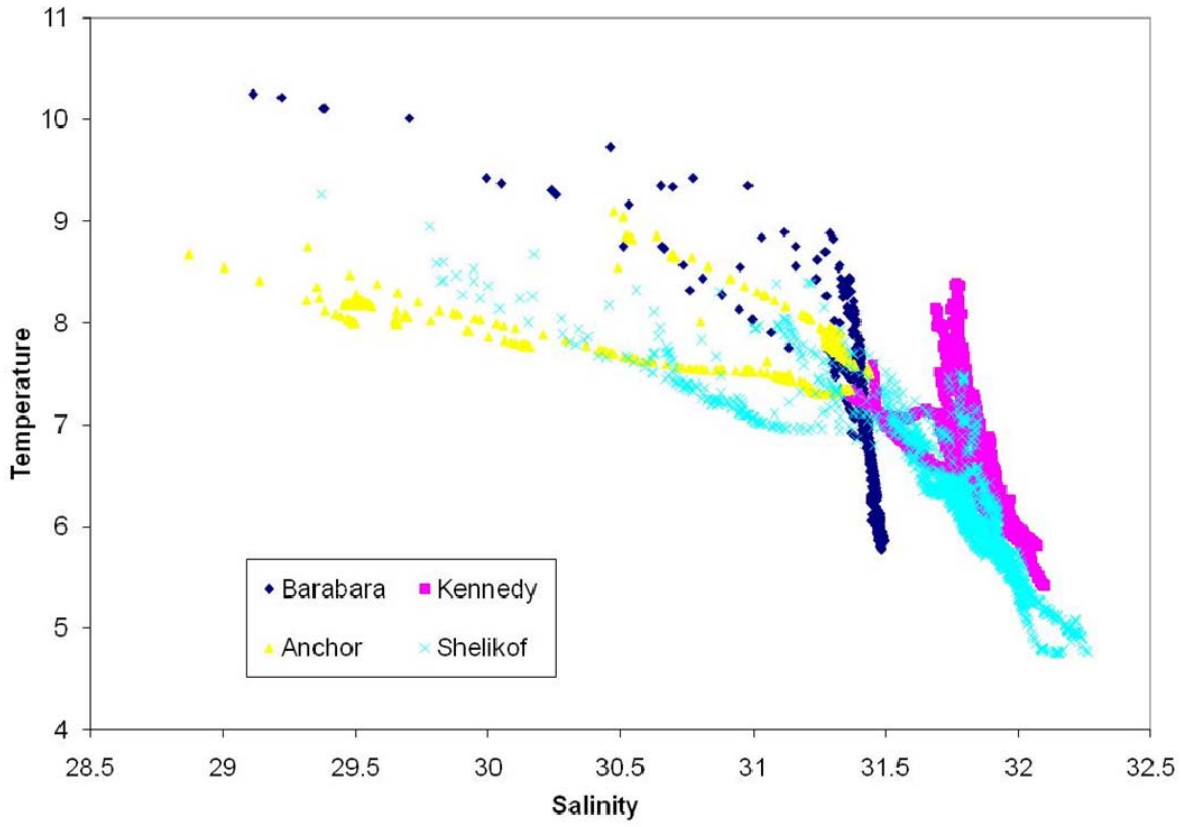

Figure 33. Sea surface temperature image of Cook Inlet is shown. The image was obtained from the Sea-Air-Land-Modeling-Observation-Network website. Note the colder waters at the confluence of Kachemak Bay and Cook Inlet, in the Barren Islands, and to the northeast of Shuyak and Afognak Islands.

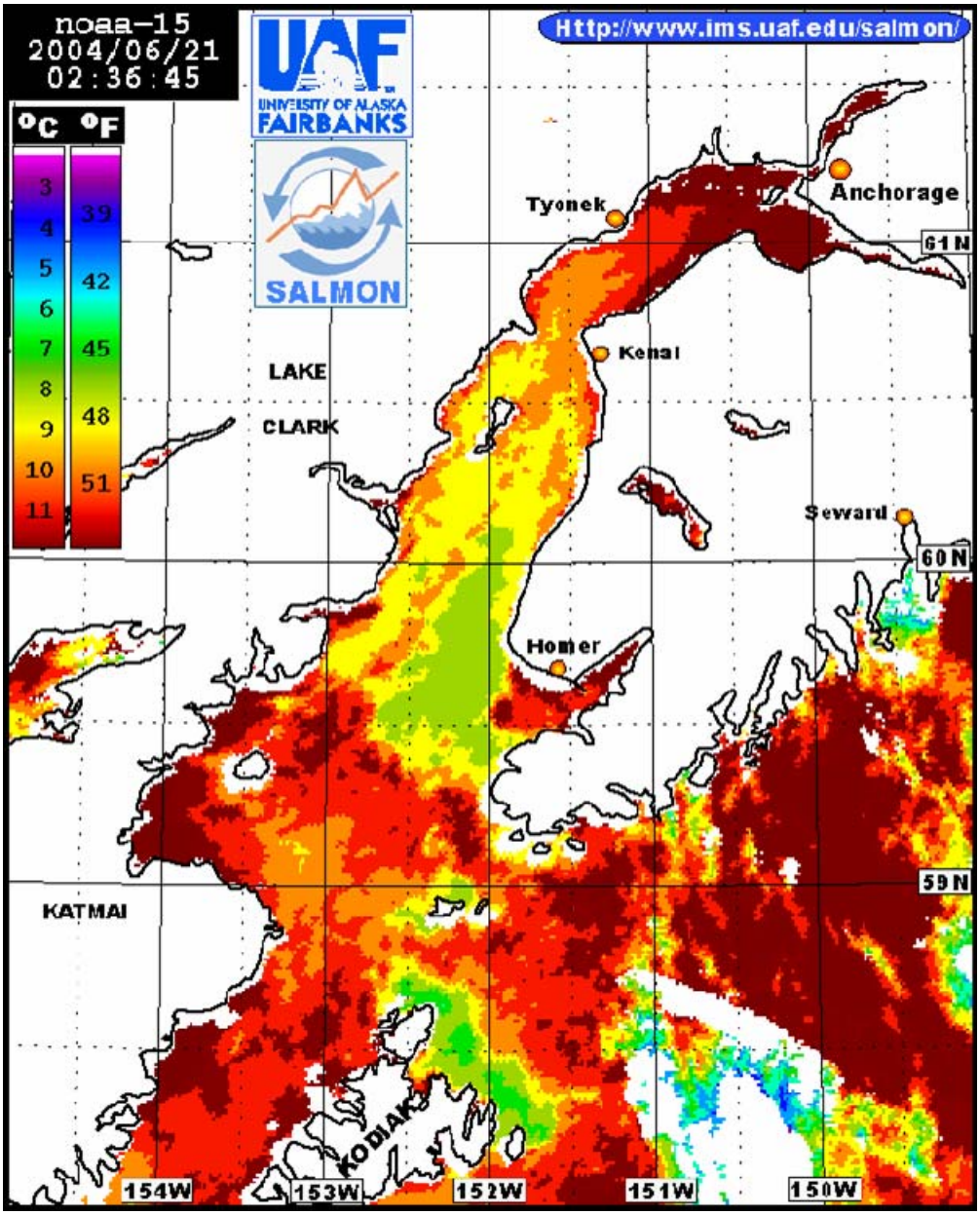

Figure 34. A SeaWiFS chlorophyll image of lower Cook Inlet is shown. Low chlorophyll values (green color) are associated with the strong mixing area at the confluence of Cook Inlet and Kachemak Bay.

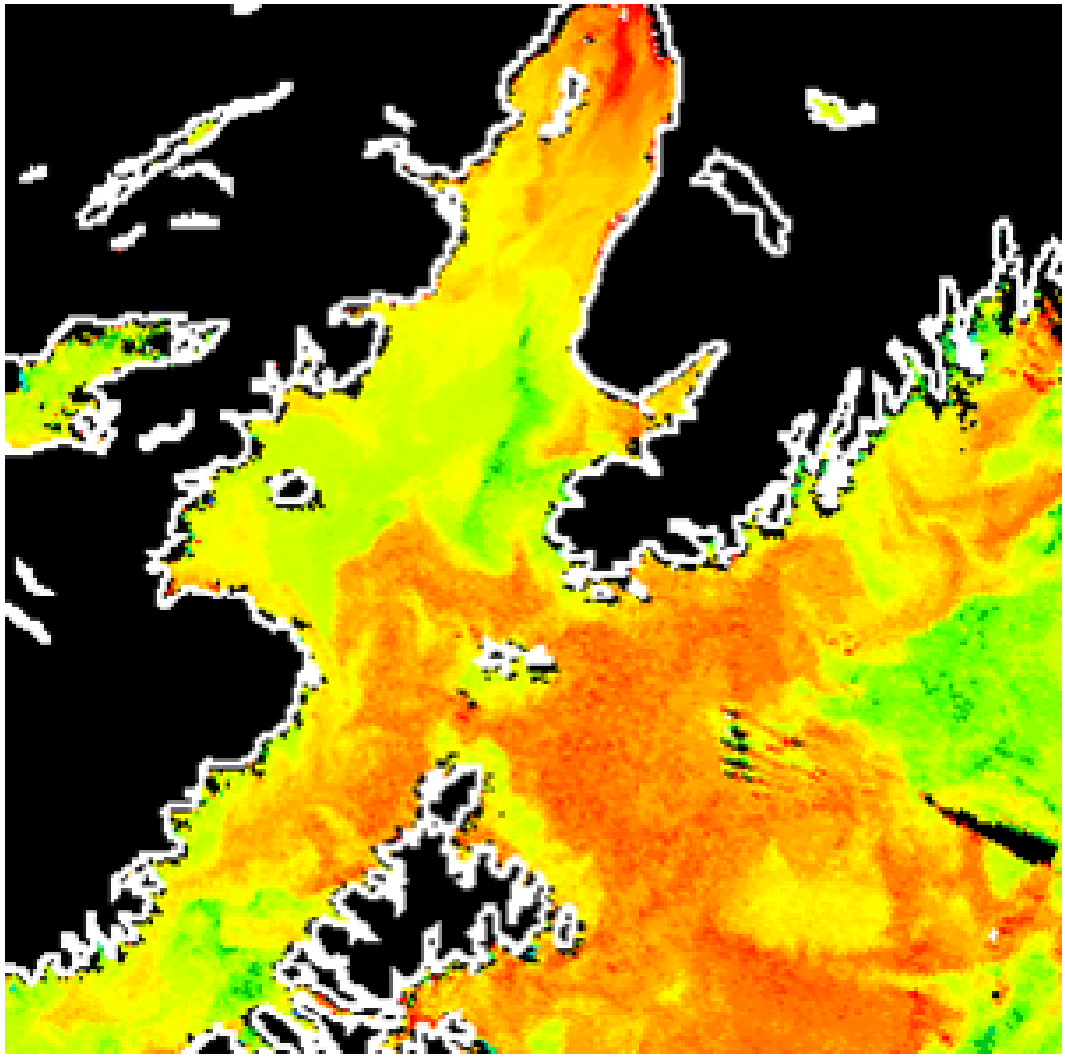

Daily surveys conducted by ADF&G showed the hydrographic structure near Anchor Point to also be modulated during the spring-neap tide cycle (Figure 28). Daily surveys conducted through July showed that the spring tides break the freshwater stratification, mixing the freshwater throughout the water column on the western side of Cook Inlet. During a neap tide when tidal mixing is relatively weak, the freshwater plume flowing along the west side of Cook Inlet is able to maintain strong stratification. Were these strong winds to persist for a few days, the stratification would likely weaken somewhat.

The hydrography of Cook Inlet varies with the semidiurnal tidal cycle, as well as the spring neap cycle. The length of the transect lines in lower Cook Inlet were too long to be able to sample fast enough to resolve semidiurnal tidal changes. Semidiurnal changes in hydrographic properties are evident in the mooring data (Figure 30). During the ebb tide, higher salinity water was carried onto the shelf east of Kennedy Entrance. The saltwater flowing onto the eastern shelf would tend to inhibit the flow of the ACC into Kennedy Entrance, suggesting there are tidally-driven pulsed intrusions of the ACC into lower Cook Inlet.

In southern Cook Inlet, in the vicinity of the Barren Islands, tidal mixing is observed in the satellite imagery and hydrographic samples. The presence of denser water adjacent to the Barren Islands would promote counter-clockwise circulation around the islands. This pattern was seen in at least one of the drifters deployed by Mark Johnson in his research of circulation in Cook Inlet (Schumacher 2005).

Remnant tidal flow around the Kodiak Island archipelago is probably the cause of the upwelling seen on the northeast side of the archipelago in the satellite imagery, and along the Shuyak end of line 1. Upwelling was observed near Shuyak Island on several occasions, even though the winds were very weak. The abundance of whales and other marine mammals observed within these upwelling areas are indicative of their ecological importance.

Our results are consistent with the findings of Burbank (1977) and Muench et al. (1978) which depict Cook Inlet exhibiting typical estuarine circulation. The dominant freshwater flows are southwestward along the western side of Cook Inlet and the ACC flowing westward across the mouth of Cook Inlet (Figure 35). Consistent with the findings of Muench et al. (1978, 1981), our results also suggest that the core of the ACC tends to follow the 100 m isobaths,

Data from drifters (http://www.pmel.noaa.gov/foci/FOCI_data.html) and our hydrographic surveys suggest that deeper water may intrude further into Cook Inlet than does the ACC. Deep waters from Shelikof Strait and Kennedy Entrance appear to be brought to the surface west of the mouth of Kachemak Bay as well as intrude north of line 3 along the eastern side of the deep channel.

Mixing resulting from the interaction of tidal currents at the confluence of Kachemak Bay and Cook Inlet may enhance this normal estuarine circulation. The presence of a denser water mass near the mouth of Kachemak Bay leads to a single counter-clockwise circulation cell near the mouth of Kachemak Bay.

It is important to recall that the upper Inlet is fresher than the lower Inlet in all seasons. The south-north salinity gradient results from more and larger streams discharging freshwater into the upper Inlet (e.g. Mantanuska River, Susitna River) compared to the lower Inlet and from the oceanic influence in the lower Inlet. The geostrophic response to the south-north salinity gradient is a westward-flowing, cross-channel baroclinic current. The strength of this cross-channel flow will necessarily vary with seasonal changes in river discharge into the Inlet. Based on earlier hydrographic surveys (Okkonen and Howell 2003) which indicate that the south-north salinity gradient within the study area is strongest between the latitudes of Kalgin Island and the Forelands, we infer that the cross-channel baroclinic current should be strongest within a few tens of kilometers south of the Forelands.

Figure 35. The inferred surface circulation pattern is shown. The light green lines represent the flow of the ACC. The dark blue lines represent the freshwater flowing down from upper Cook Inlet. Dashed lines represent weak or intermittent flow paths. The light blue line is freshwater leaving Kachemak Bay. The light boxes are areas with persistent upwelling or strong mixing, and the red lines are gyres set up in part by the upwelling areas.

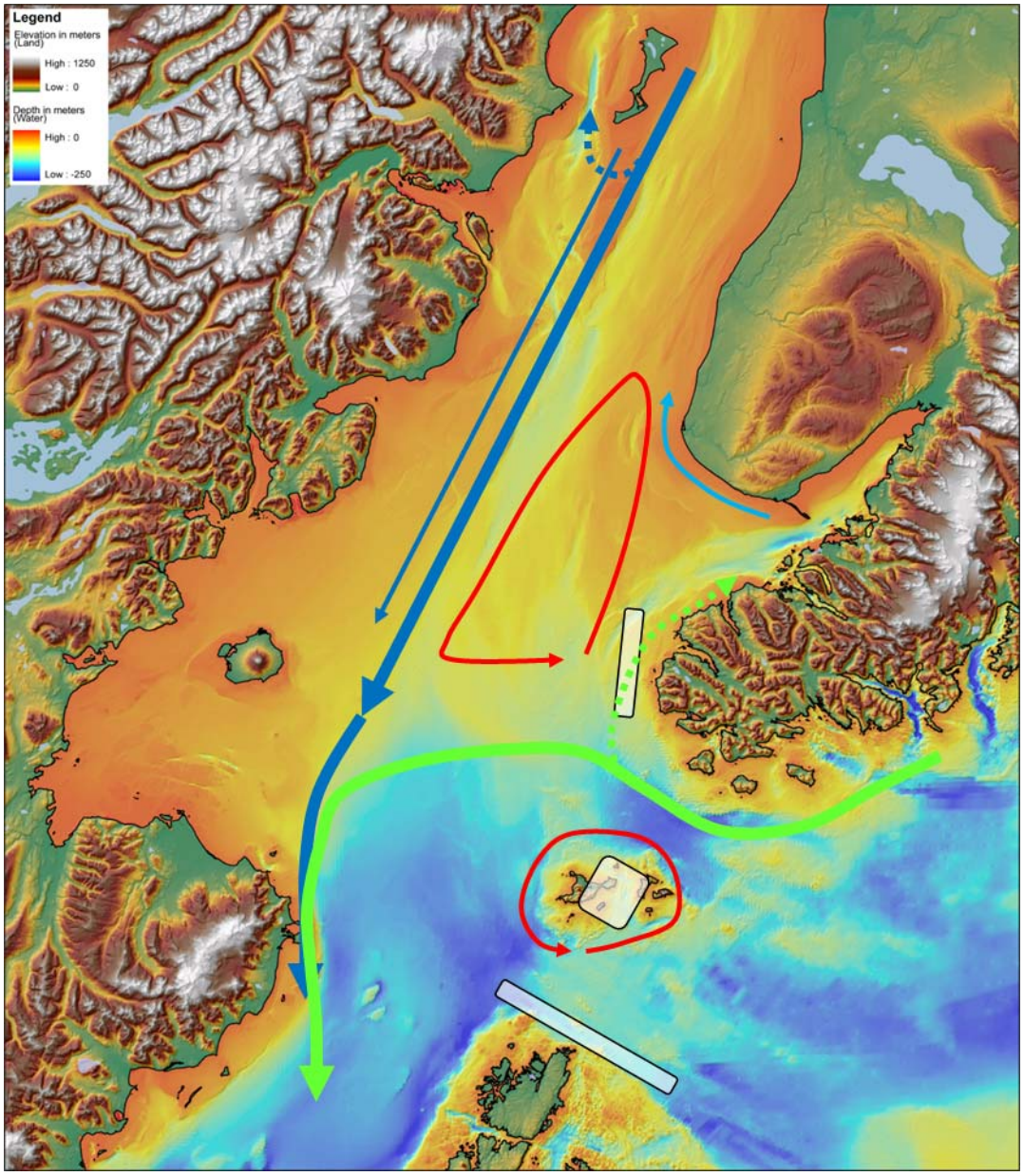

SUMMARY

Changes in solar heating provide a strong seasonal cycle to the oceanographic properties of Cook Inlet. More importantly, the seasonal change in freshwater flowing down Cook Inlet, and into Cook Inlet as the ACC alter the strength of currents and the exchange of water within the region. The water properties are also highly dependent on the tides. Significant mixing, due to the large tides in the area, influences the location and strength of salinity gradients and, hence, the location and strength of the geostrophic baroclinic currents. The modulation of that mixing during the spring-neap cycle alters the path of the ACC and the exchange of water between Cook Inlet and Kachemak Bay.

Temperature and salinity gradients exist between lower and central Cook Inlet, between the east and west sides of the Inlet, and are evident in the hydrographic data acquired through this project. Based on our observations we suggest that there are five principal factors necessary for accurate numerical simulations of Cook Inlet hydrography and circulation. These conditions include accurate spatial and/or temporal representations of (1) freshwater discharges into Cook Inlet (e.g. Susitna River, Matanuska River, Kenai River, and other Cook Inlet river discharges, plus precipitation), (2) heat and salt fluxes through Kennedy Entrance (including ACC transport), Stevenson Entrance, Shelikof Strait, (3) bathymetry, (4) tidal forcing and (5) solar insolation. Although wind forcing is also an important forcing mechanism, it was not directly investigated as part of this project, nor its role readily discernable from the hydrographic data.

With respect to numerically modeling circulation in Cook Inlet, the minimum time and space scales to be resolved are those associated with the semidiurnal tide (12.4 hr) and the steep bathymetric slopes. This implies a maximum time step of an hour or two and a spatial grid of ~100 m or less.

Several questions remain to be resolved. What is the role of the winds in altering stratification and the path of the major currents? How closely does the seasonal freshwater signal along the west side of Cook Inlet resemble the ‘step function’ discharge profile characteristic of upper Cook Inlet rivers? What are the mixing rates in different areas of Cook Inlet, and what regions have the strongest upwelling? What are the circulation patterns in Kamishak Bay? We hope that other measurement programs that are in progress or recently completed will help to answer these questions.

ACKNOWLEDGMENTS

We thank the Minerals Management Service and the Coastal Marine Institute (University of Alaska Fairbanks) for funding this project. We acknowledge the effort of the captains and crews of several vessels Rolfy, Kittiwake, Waters, Columbia, Corrina Kay, and Americanus that supported the CTD surveys of lower Cook Inlet. A special thanks goes to John Crosbie for help in determining a suitable location for the lower Cook Inlet mooring and effort as part of several of the hydrographic surveys. We thank Steve Tvenstrup and Eric Huebsch for their help with the hydrographic surveys near the Forelands, and Scott Griffith with XTO Energy for deploying a mooring on their platform.

STUDY PRODUCTS

Pegau, W.S. 2004. Circulation into Kachemak Bay: Does it affect crab populations. Presentation at the Interagency Crab Meeting, December 2004, Anchorage, AK

Okkonen, S. 2005. Hydrography of Central Cook Inlet: August 2003. In: Cook Inlet Physical Oceanography Workshop Proceedings, (http://doc.aoos.org/other_meetings/2005/cook_inlet_physical_oceanography_workshop_proceedings-combined%20sections-final-2006.pdf). J. Schumacher [ed].

Pegau, W.S., S. Saupe, S. Okkonen, and M. Willette (S. Pegau presenter). 2005. Hydrography of lower Cook Inlet. In: Cook Inlet Physical Oceanography Workshop Proceedings (http://doc.aoos.org/other_meetings/2005/cook_inlet_physical_oceanography_workshop_proceedings-combined%20sections-final-2006.pdf). J. Schumacher [ed].

Pegau, W.S. 2005. Satellite tools for Cook Inlet. In: Cook Inlet Physical Oceanography Workshop Proceedings (http://doc.aoos.org/other_meetings/2005/cook_inlet_physical_oceanography_workshop_proceedings-combined%20sections-final-2006.pdf). J. Schumacher [ed].

Pegau, W.S., S. Okkonen, and S. Saupe (S. Pegau presenter). 2006. Seasonality of boundary conditions for Cook Inlet, Alaska. Presentation to CMI Annual Research Review, 14 February 2006, Fairbanks, AK.

Pegau, W.S., E. Cokelet, and S. Saupe. 2006. Oceanographic boundary conditions to Cook Inlet. Presentation at 2006 Symposium: Marine Science in Alaska, January 22-25, 2006. Anchorage, AK.

Baird, S., and W.S. Pegau. 2006. Water flow into Kachemak Bay: Is it isolated? Poster presented at the Ocean Sciences meeting, February 20-24, 2006. Honolulu, HI.

Pegau, W.S. 2006. What's new in the bay. Presentation of research being conducted at the Kachemak Bay Research Reserve given to Alaska Department of Fish and Game leadership, NERR Stewardship Coordinators, and several others.

Pegau, W.S. 2007. Connecting oceanography and fisheries in the offshore test fishing program. Poster presented at the Alaska Marine Science Symposium. January 24, 2007. Anchorage. Alaska.

Pegau, W.S., S. Okkonen, and S. Saupe (S. Pegau presenter). 2007. Seasonality of boundary conditions for Cook Inlet, Alaska. Presentation to CMI Annual Research Review, February 6, 2007, Fairbanks, AK.

REFERENCES

Barrick, D.E. 1978. HF Surface-current mapping radar 1977 Alaskan operations – lower Cook Inlet. In: Environmental Assessment of the Alaskan Continental Shelf. Annual Reports. 39pp.

Burbank, D.C. 1977. Circulation studies in Kachemak Bay and Lower Cook Inlet. In Environmental Studies of Kachemak Bay and Lower Cook Inlet. Trasky, LL., L.B. Flagg. and D.C. Burbank eds. vol III. 207 pp.

Johnson, M.A., and S.R. Okkonen [eds.]. 2000. Proceedings Cook Inlet Oceanography Workshop. November 1999, Kenai, AK. Final Report. OCS Study MMS 2000-043. University of Alaska Coastal Marine Institute, University of Alaska Fairbanks and USDOI, MMS, Alaska OCS Region. 118 p.

MMS (Minerals Management Service) EIS. 2003. Final Environmental Impact Statement Cook Inlet Planning Area Oil and Gas Lease Sales 191 and 199. OCS EIS/EA MMS 2003-055: Volume I. 702 pp. and Volume III. 363 pp.

Muench, R.D., H.O. Mofjeld, and R.L. Charnell. 1978. Oceanographic conditions in Lower Cook Inlet: Spring and Summer 1973. Journal of Geophysical Research. 83: 5090-5098.

Muench, R.D., J.D. Schumacher, and C.A. Pearson. 1981. Circulation in the lower Cook Inlet, Alaska. NOAA Technical Memorandum ERL PMEL-28. Seattle. 26 pp.

Oey, L.Y., T. Ezer, C. Hu, and F.E. Muller-Karger. 2007. Baroclinic tidal flows and inundation processes in Cook Inlet, Alaska: numerical modeling and satellite observations, Ocean Dynamics, 57: 205-211.

Okkonen, S.R. 2004. Observations of hydrography and currents in central Cook Inlet, Alaska during diurnal and semidiurnal tidal cycles. OCS Study MMS 2004-058, University of Alaska Coastal Marine Institute, University of Alaska Fairbanks and USDOI, MMS, Alaska OCS Region, 27 p.

Okkonen, S.R. and S.S. Howell. 2003. Measurements of temperature, salinity, and circulation in Cook Inlet, Alaska. Final Report. OCS Study MMS 2003-036, University of Alaska Coastal Marine Institute, University of Alaska Fairbanks and USDOI, MMS, Alaska OCS Region, 28 p.

Royer, T.C. 1982. Coastal fresh water discharge in the Northeast Pacific. Journal of Geophysical Research. 87:2017-2021.

Royer, T.C. 2005. Hydrographic responses at a coastal site in the northern Gulf of Alaska to seasonal and interannual forcing. Deep-Sea Research Part II-Topical Studies in Oceanography, 52**:**267-288.

Schumacher, J.D. [ed.]. 2005. Cook Inlet Physical Oceanography Workshop Proceedings (http://doc.aoos.org/other_meetings/2005/cook_inlet_physical_oceanography_workshop_proceedings-combined%20sections-final-2006.pdf)

Speckman, S.G., J.F. Piatt, C.V. Minte-Vera, and J.K. Parrish. 2005. Parallel structure among environmental gradients and three trophic levels in a subarctic estuary. Progress in Oceanography. 66: 25-65.

Weingartner, T.J., S.L. Danielson, and T.C. Royer. 2005. Freshwater variability and predictability in the ACC. Deep-Sea Research Part II-Topical Studies in Oceanography, 52**:** 169-191.

APPENDICES

Appendix 1. Station locations

Line	Station	Lon (°W)	Lat (°N)	Water Depth
1	1	151.875	59.203	33
1	2	151.890	59.190	40
1	3	151.905	59.177	38
1	4	151.920	59.157	71
1	5	151.952	59.122	123
1	6	151.983	59.087	199
1	7	152.015	59.052	202
1	8	152.047	59.020	217
1	9	152.078	58.988	125
1	10	152.110	58.957	57
1	11	152.142	58.925	84
1	12	152.167	58.893	73
1	13	152.187	58.862	88
1	14	152.207	58.830	124
1	15	152.227	58.798	121
1	16	152.247	58.767	120
1	17	152.267	58.735	122
1	18	152.287	58.703	123
1	19	152.298	58.690	89
1	20	152.310	58.677	143
1	21	152.322	58.663	137
1	22	152.333	58.650	103
2	23	152.633	58.613	32
2	24	152.662	58.623	54
2	25	152.685	58.635	94
2	26	152.707	58.643	218
2	27	152.767	58.665	194
2	28	152.817	58.687	164
2	29	152.868	58.703	161
2	30	152.920	58.722	146
2	31	152.973	58.742	153
2	32	153.027	58.760	178
2	33	153.080	58.780	169
2	34	153.133	58.789	195
2	35	153.158	58.812	202
2	36	153.187	58.820	180
2	37	153.213	58.830	113
2	38	153.240	58.838	35
3	39	152.567	60.007	24
3	40	152.537	59.997	32
3	41	152.510	59.987	35
3	42	152.482	59.987	33
3	43	152.422	59.957	27
3	44	152.368	59.938	52
3	45	152.308	59.918	112
3	46	152.253	59.900	82
3	47	152.200	59.880	73
3	48	152.145	59.863	52
3	49	152.093	59.845	40
3	50	152.040	59.827	38
3	51	151.987	59.810	35
3	52	151.958	59.798	29
3	53	151.935	59.790	22
3	54	151.905	59.780	14
3	55	151.883	59.772	12
4	56	151.650	59.492	21
4	57	151.650	59.508	102
4	58	151.650	59.525	107
4	59	151.650	59.542	86
4	60	151.650	59.558	76
4	61	151.650	59.575	63
4	62	151.650	59.592	35
4	63	151.650	59.608	29
4	64	151.650	59.625	27
4	65	151.650	59.492	10

Line	Station	Lon (°W)	Lat (°N)	Water Depth (m)
5	1c	151.417	60.717	38
5	2c	151.450	60.717	24
5	3c	151.483	60.717	21
5	4c	151.517	60.717	26
5	5c	151.550	60.717	29
5	6c	151.583	60.717	61
5	7c	151.617	60.717	124
5	8c	151.650	60.717	29
5	9c	151.683	60.717	9
6	90	151.925	59.212	36
6	91	151.952	59.205	52
6	92	151.980	59.197	104
6	93	152.007	59.190	106
6	94	152.062	59.175	105
6	96	152.172	59.147	125
6	97	152.227	59.132	132
6	98	152.282	59.118	127
6	99	152.335	59.103	96
6	100	152.390	59.088	113
6	101	152.445	59.075	140
6	102	152.500	59.060	132
6	103	152.555	59.045	138
6	104	152.610	59.030	151
6	105	152.665	59.017	155
6	106	152.720	59.002	164
6	107	152.773	58.988	175
6	108	152.828	58.973	179
6	109	152.883	58.958	175
6	110	152.938	58.945	169
6	111	152.993	58.930	167
6	112	153.048	58.915	167
6	113	153.103	58.902	170
6	114	153.158	58.887	175
6	115	153.185	58.880	171
6	116	153.212	58.872	129
6	117	153.240	58.865	32
7	66	153.302	59.350	28
7	67	153.268	59.348	42
7	68	153.237	59.355	46
7	69	153.172	59.347	50
7	70	153.107	59.343	50
7	71	153.042	59.342	53
7	72	152.977	59.340	56
7	73	152.912	59.338	72
7	74	152.847	59.335	77
7	75	152.782	59.333	75
7	76	152.717	59.332	71
7	77	152.652	59.330	72
7	78	152.585	59.327	72
7	79	152.520	59.325	70
7	80	152.455	59.323	71
7	81	152.390	59.320	85
7	82	152.325	59.318	88
7	83	152.260	59.317	82
7	84	152.196	59.315	81
7	85	152.130	59.313	85
7	86	152.097	59.312	76
7	87	152.065	59.310	77
7	88	152.032	59.310	50
7	89	152.000	59.308	27

Appendix 2. Cruise dates

Central Cook Inlet cruises were completed within a few hours. The lower Cook Inlet cruises in 2004 and 2005 required 48 hours to complete. In 2006 the additions of lines 6 and 7 made it so that 72 hours were needed to complete the survey. Dates of cruises are the starting date.

Central	Lower
21-May-04	18-Apr-04
24-Jun-04	25-May-04
8-Aug-04	13-Jun-04
17-Sep-04	17-Jul-04
9-Oct-04	16-Aug-04
	7-Sep-04
30-Mar-05	8-Jan-05
2-May-05	25-Apr-05
1-Jun-05	14-Jun-05
26-Aug-05	28-Jul-05
3-Oct-05	4-Sep-05
	13-Oct-05
9-Aug-06	26-Jul-06
	5-Aug-06
	12-Aug-06
	11-Sep-06

The Department of the Interior Mission

As the Nation's principal conservation agency, the Department of the Interior has responsibility for most of our nationally owned public lands and natural resources. This includes fostering sound use of our land and water resources; protecting our fish, wildlife, and biological diversity; preserving the environmental and cultural values of our national parks and historical places; and providing for the enjoyment of life through outdoor recreation. The Department assesses our energy and mineral resources and works to ensure that their development is in the best interests of all our people by encouraging stewardship and citizen participation in their care. The Department also has a major responsibility for American Indian reservation communities and for people who live in island territories under U.S. administration.

The Minerals Management Service Mission

As a bureau of the Department of the Interior, the Minerals Management Service's (MMS) primary responsibilities are to manage the mineral resources located on the Nation's Outer Continental Shelf (OCS), collect revenue from the Federal OCS and onshore Federal and Indian lands, and distribute those revenues.

Moreover, in working to meet its responsibilities, the **Offshore Minerals Management Program** administers the OCS competitive leasing program and oversees the safe and environmentally sound exploration and production of our Nation's offshore natural gas, oil and other mineral resources. The MMS **Royalty Management Program** meets its responsibilities by ensuring the efficient, timely and accurate collection and disbursement of revenue from mineral leasing and production due to Indian tribes and allottees, States and the U.S. Treasury.

The MMS strives to fulfill its responsibilities through the general guiding principals of: (1) being responsive to the public's concerns and interests by maintaining a dialogue with all potentially affected parties and (2) carrying out its programs with an emphasis on working to enhance the quality of life for all Americans by lending MMS assistance and expertise to economic development and environmental protection.